Nematostatics of triple lines

Alejandro D. Rey
Department of Chemical Engineering, McGill University, 3610 University Street, Montreal, Quebec, Canada H3A 2B2

(Received 24 June 2002; published 30 January 2003)

The Landau–de Gennes model for nematic liquid crystal bulk and interfaces has been extended to nematic triple lines involving the intersection of two isotropic fluids and one nematic liquid crystalline phase. A complete set of bulk, interface, and triple line force and torque balance equations has been formulated. The triple line force and torque balance equations have linear, interfacial, and bulk contributions. The bulk contributions appear as junction integrals, the surface contributions as junctions sums, and the line contributions as gradients of stresses. Reduction of dimensionality from three to one dimensional creates the following effects: (a) bulk terms enter interfacial balances as surface jumps and line balances as junction integrals, and (b) surface terms enter linear balances as junction sums. Line stress and torque equations are derived using classical liquid crystal models. The correspondence between line stress and line torque and their surface and bulk analogs is established. The triple line force and torque balance equations are use to analyze the contact angle in a nematic lens lying at the interface between two isotropic fluids, when the prefered surface orientation is tangential. The effect of anisotropy and long range elasticity on triple line phases is established. Under weak anchoring the contact angle is shown to be a function of the anchoring energy at the nematic-isotropic interface, while under strong anchoring conditions the contact angle is a function of the Peach-Koehler force that originates from bulk long range elasticity and acts on the triple line. The use of the complete set of balance equations removes the classical inconsistency in force balances at a contact line by properly taking into account long range (bulk gradient elasticity) and anisotropic (interfacial anchoring elasticity) effects.

DOI: 10.1103/PhysRevE.67.011706 PACS number(s): 61.30.−v

I. INTRODUCTION

The surface physics of nematic liquid crystals is currently an active area of research [1–6] since many applications of liquid crystalline materials involve multiphase systems, where interfaces play significant roles. Interfacial orientation phenomena and orientational transitions in fixed geometries are well characterized experimentally [1–3] and theoretically [4–7]. On the other hand, deforming soft nematic interphases are less well understood. Furthermore, wetting, spreading, flotation, foaming, and fluid-liquid crystal displacement are examples where contact lines are present [8,9]. At present the understanding and characterization of contact lines involving nematic phases is starting to be developed [10–12]. This paper presents a contribution to the formulation of models of systems displaying bulk, surface, and triple line phases. In particular, we focus on a representative system of three bulk phases, three interfaces, and one triple line, which arises when two isotropic fluid phases intersect a nematic phase. A typical example is a nematic droplet or lens suspended at the interface between two isotropic fluids. Generalizations to other triple lines, such as those arising at the intersection of solid isotropic and fluid nematic liquid crystal phases can be made following the procedure presented in this paper.

Fluid triple lines arising from the intersection of three isotropic fluids are described by the Neumann equation [8], which is a force balance of tangential forces acting along the three interfaces. The tangential forces at the triple line arise because the surface stress tensor is a tangential tensor field, indicating only the presence of normal (tension) stresses [8,9]. Since liquid crystal interfaces are anisotropic, the surface stress tensor is not a tangential tensor field, indicating that, in addition to normal stresses, there are bending stresses and distortion shear stresses [13]. Bending stresses at the nematic triple line result in forces that are not tangential such that force balances in any direction can be accomplished [12]. When considering solid triple lines that arise from the intersection of two fluid phases and a flat solid substrate the contact angle is given by the Young equation [8,9]. When neglecting distortions in the solid substrate it is found that a model based on tangential stresses is not able to balance forces along the normal to the solid surface [9]. In the present model we show that forces at a triple line may balance in all directions since stresses are not tangential tensors.

Force balances at a triple line, as in the Neumann and Young equations, are used to model isotropic systems [8,9]. On the other hand, for anisotropic nematic liquid crystalline materials force balances and torque balances are required. Modeling of anisotropic surfaces using force and torque balances is very common in metallurgical [15,16], thin membrane, and film [17,18] and liquid crystalline systems [13,19]. The need to use both force and torque balances is not restricted to dimensionality (three and two dimensional), and carries over to anisotropic triple lines. This was first recognized in [20]. Bulk, surface, and line force and torque balance equations under the coexistence of bulk, interface, and line phases give the complete set of equations in the presence of anisotropy. In addition to anisotropy, nematic liquid crystals display long range elasticity [14]. The bulk and surface long range elasticity have been used to model many observed phenomena (see for example, [1–7,14,21]). It is therefore possible that endowing a nematic triple line also with long range elasticity will assist in providing further mechanisms for wetting and wetting transitions [22,23].

The tensorial Landau–de Gennes force and torque balance equations of nematic liquid crystals for surface phenomena have been presented and used extensively (see, for example, [3,13,24]). On the other hand there are few applications to contact line problems. In [10] a two-dimensional (2D) force balance equation for solid contact lines was formulated and used to model wetting processes in the absence of line tension effects. In this work [10] the role of bulk long range elasticity on the line force balance was established. The vectorial Frank-Oseen force and torque balance equations of nematic liquid crystals have been formulated for solid contact lines in the absence of long range energy [20]. The force and torque balance equations at cusps using the vectorial Frank-Oseen model have been formulated and used to establish stability criteria [6].

The objectives of this paper are as follows. (1) To present a complete set of Landau–de Gennes equations for nematic liquid crystals for coexisting bulk, surface, and line phases, that include force and torque balances, using generalized bulk, surface, and line energies that have homogeneous and long range contributions. (The presence of similar energies in the three phases allows for a systematic formulation of stress and torque equations as well as providing a unified approach at developing the force and torque balance equations.) (2) To establish the effect of anisotropy and long range energies on the forces and torques at the triple line phase.

The organization of this paper is as follows. Section II defines the geometry, the nematic order parameter, and the nematic elasticities, and derives the balance equations and constitutive equations for bulk, surface, and line stresses and torques. Section III develops the force and torque balance equations in the Frenet-Serret frame of the triple line. Section IV presents the applications to a nematic lens between two isotropic fluids under weak and strong anchoring conditions. Section V presents the conclusions.

II. BALANCE EQUATIONS

A. Geometry and order in nematic bulk, interface, and triple line phases

In this paper we analyze the statics of a nematic triple line, denoted by C^{tl}, that arises at the intersection of two isotropic phases and a nematic phase. The geometry is shown in Fig. 1. The nematic bulk region is R^1 and the isotropic bulk regions are R^2 and R^3. The total bulk region R is the union of the three bulk regions: $R=R^1+R^2+R^3$. The outer bounding surfaces of the three bulk region are, respectively, S^1, S^2, and S^3. The outward bounding surface of R is S and is the union of the three surfaces: $S=S^1+S^2+S^3$. The surface of discontinuity between R^1 and R^2 is $\Sigma^{(1,2)}$, that between R^3 and R^1 is $\Sigma^{(3,1)}$, and that between R^3 and R^2 is $\Sigma^{(2,3)}$. The union of the three surfaces of discontinuity is $\Sigma=\Sigma^{(1,2)}+\Sigma^{(3,1)}+\Sigma^{(2,3)}$. The outer bounding edge of $\Sigma^{(1,2)}$ is $C^{(1,2)}$, that of $\Sigma^{(3,1)}$ is $C^{(3,1)}$, and that of $\Sigma^{(2,3)}$ is $C^{(2,3)}$. The intersection of the surface of discontinuity Σ and the bounding surfaces S is $C=C^{(1,2)}+C^{(3,1)}+C^{(2,3)}$. The triple line C^{tl} is the common intersection of $\Sigma^{(1,2)}$, $\Sigma^{(3,1)}$, and $\Sigma^{(2,3)}$. The intersections of the triple line C^{tl} and S are two end points $E^{\mathrm{tl}(s)}$ and $E^{\mathrm{tl}(e)}$, where s indicates the start and e the end. The total bounding surface for the nematic phase is $S^n=\Sigma^{(1,2)}+\Sigma^{(3,1)}+S^1$. The unit vector $\boldsymbol{\xi}^{(i,j)}$ is the normal to the interface of discontinuity $\Sigma^{(i,j)}$ and is directed from R^j into R^i. The outward unit normal to $C^{(i,j)}$ is $\boldsymbol{\mu}^{(i,j)}$. The unit vector normal to the triple line C^{tl}, tangent to $\Sigma^{(i,j)}$, and directed away from C^{tl} is $\boldsymbol{\nu}^{(i,j)}$. The two unit tangents to the triple line C^{tl} at $E^{\mathrm{tl(s)}}$ and $E^{\mathrm{tl(e)}}$ pointing away from C^{tl} are $\boldsymbol{\alpha}^{(s)}$ and $\boldsymbol{\alpha}^{(e)}$. The outward unit normal to S^i is $\boldsymbol{\nu}^{(i)}$. When no ambiguity arises we drop superscripts.

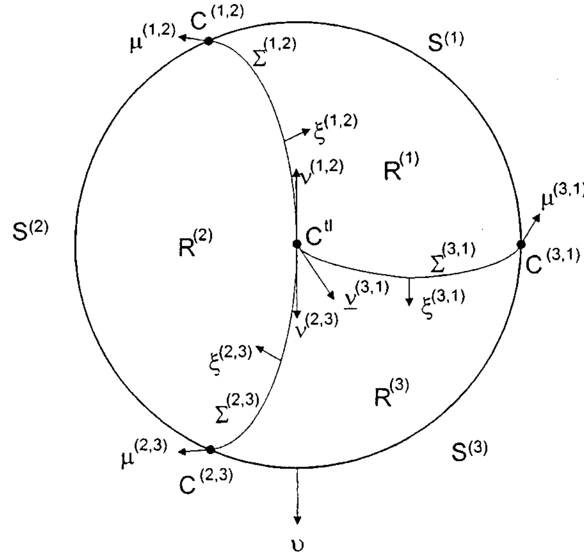

FIG. 1. Schematic of the coexistence of three bulk, three interface, and one triple line phases. The nematic bulk region is R^1 and the isotropic bulk regions are R^2 and R^3. The total bulk region R is the union of the three bulk regions: $R=R^1+R^2+R^3$. The outer bounding surfaces of the three bulk region are, respectively, S^1, S^2, and S^3. The outward bounding surface of R is S and is the union of the three surfaces: $S=S^1+S^2+S^3$. The surface of discontinuity between R^1 and R^2 is $\Sigma^{(1,2)}$, between R^3 and R^1 is $\Sigma^{(1,2)}$, and between R^3 and R^2 is $\Sigma^{(3,2)}$. The union of the three surfaces of discontinuity is $\Sigma=\Sigma^{(1,2)}+\Sigma^{(3,1)}+\Sigma^{(2,3)}$. The outer bounding edge of $\Sigma^{(1,2)}$ is $C^{(1,2)}$, the outer bounding edge of $\Sigma^{(3,1)}$ is $C^{(3,1)}$, and of $\Sigma^{(2,3)}$ is $C^{(2,3)}$. The intersection of the surface of discontinuity Σ and the bounding surfaces S is $C=C^{(1,2)}+C^{(3,1)}+C^{(2,3)}$. The triple line C^{tl} is the common intersection of $\Sigma^{(1,2)}$, $\Sigma^{(3,1)}$, and $\Sigma^{(2,3)}$. The intersections of the triple line C^{tl} and S are two end points $E^{\mathrm{tl}(s)}$, and $E^{\mathrm{tl}(e)}$, where s indicates the start, and e the end. The total bounding surface for the nematic phase is $S^n=\Sigma^{(1,2)}+\Sigma^{(3,1)}+S^1$. The unit vector $\boldsymbol{\xi}^{(i,j)}$ is the normal to the interface of discontinuity $\Sigma^{(i,j)}$ and is directed from R^j into R^i. The outward unit normal to $C^{(i,j)}$ is $\boldsymbol{\mu}^{(i,j)}$. The unit vector normal to the triple line C^{tl}, tangent to $\Sigma^{(i,j)}$, and directed away from C^{tl} is $\boldsymbol{\nu}^{(i,j)}$. The two unit tangents to the triple line C^{tl} at $E^{\mathrm{tl}(s)}$ and $E^{\mathrm{tl}(e)}$ pointing away from C^{tl} are $\alpha^{(s)}$ and $\alpha^{(e)}$. The outward unit normal to S^i is $\boldsymbol{\nu}^{(i)}$. The orientation of the triple line is given by the unit vector **t**. Rotation of a right-handed screw in a clockwise direction advances the screw in the direction of **t**.

The geometry of each interface ($\Sigma^{(i,j)}$) is characterized by a mean surface curvature $H^{(i,j)}$ given by [8,9]

$$H^{(i,j)}=-\frac{1}{2}\nabla_s\cdot\boldsymbol{\xi}^{(i,j)}=\frac{1}{2}\mathbf{I}_s^{(i,j)}:\boldsymbol{\beta}_s^{(i,j)}=-\frac{1}{2}\mathbf{I}_s^{(i,j)}:\nabla_s\boldsymbol{\xi}^{(i,j)}$$
$$=\frac{1}{2}(\chi_1^{(i,j)}+\chi_2^{(i,j)}),\tag{1a}$$

$$\boldsymbol{\beta}_s^{(i,j)}=-\nabla_s\boldsymbol{\xi}^{(i,j)}=\chi_1^{(i,j)}\mathbf{e}_1^{(i,j)}\mathbf{e}_1^{(i,j)}+\chi_2^{(i,j)}\mathbf{e}_2^{(i,j)}\mathbf{e}_2^{(i,j)},$$
$$(i,j)=(1,2),(3,1),(2,3),\tag{1b}$$

where for each interface $\Sigma^{(i,j)}$ $\nabla_s=\mathbf{I}_s^{(i,j)}\cdot\nabla$ is the surface gradient, $\mathbf{I}_s^{(i,j)}=\mathbf{I}-\boldsymbol{\xi}^{(i,j)}\boldsymbol{\xi}^{(i,j)}$ is the 2×2 unit surface dyadic for interface (i,j), $\mathbf{I}$ is the 3×3 unit dyadic, $\boldsymbol{\beta}_s^{(i,j)}$ is the 2×2 symmetric surface curvature dyadic, and $\{\chi_m^{(i,j)}\}$ and $\{\mathbf{e}_m^{(i,j)}\}$, $m=1,2$ are the eigenvalues and eigenvectors of $\boldsymbol{\beta}_s^{(i,j)}$. The divergence of $\mathbf{I}_s^{(i,j)}$ is a normal vector: $\nabla_s\cdot\mathbf{I}_s^{(i,j)}=2H^{(i,j)}\boldsymbol{\xi}^{(i,j)}$. The symmetric surface curvature dyadic $\boldsymbol{\beta}_s^{(i,j)}$ is given in terms of mutually perpendicular unit vectors $(\mathbf{e}_1^{(i,j)},\mathbf{e}_2^{(i,j)})$ in the directions of the principal axes of curvature. The principal curvatures $(\chi_1^{(i,j)},\chi_2^{(i,j)})$ of the surface are defined by $\boldsymbol{\beta}_s^{(i,j)}\cdot\mathbf{e}_m^{(i,j)}=\chi_m^{(i,j)}\mathbf{e}_m^{(i,j)}$, $i=1,2$. Finally, another common way to express the principal curvatures $(\chi_1^{(i,j)},\chi_2^{(i,j)})$ is in terms of the principal radii of curvature $(r_m^{(i,j)})$, as follows: $\chi_m^{(i,j)}=-1/r_m^{(i,j)}$, $m=1,2$.

To describe the geometry of the triple line C^{tl} we use the Frenet-Serret formulas. The principal frame is $(\mathbf{t},\mathbf{p},\mathbf{b})$, where $\mathbf{t}=\mathbf{p}\times\mathbf{b}$ is the unit tangent, $\mathbf{p}=\mathbf{b}\times\mathbf{t}$ is the unit principal normal, and $\mathbf{b}=\mathbf{t}$ is the binormal unit vector. Representing the contact line by $\mathbf{r}=\mathbf{r}(s)$, the curvature κ and the torsion τ are

$$\frac{d}{ds}\begin{bmatrix}\mathbf{t}\\ \mathbf{p}\\ \mathbf{b}\end{bmatrix}=\begin{bmatrix}0 & \varkappa & 0\\ -\varkappa & 0 & \tau\\ 0 & -\tau & 0\end{bmatrix}\begin{bmatrix}\mathbf{t}\\ \mathbf{p}\\ \mathbf{b}\end{bmatrix}.\tag{2}$$

The unit line dyad is $\mathbf{I}_\ell=\mathbf{tt}$. The line gradient operator is given by $\nabla_\ell(\cdot)=\mathbf{I}_\ell\cdot\nabla(\cdot)$. The divergence of the unit dyad is $\nabla_\ell\cdot\mathbf{I}_\ell=\varkappa\mathbf{p}$. The linear curvature dyadic $\boldsymbol{\beta}_\ell$ is given by

$$\beta_\ell=-\nabla_\ell\mathbf{p}=\varkappa\mathbf{tt}\tag{3}$$

and the line curvature by

$$\varkappa=-\nabla_\ell\cdot\mathbf{p}=\mathbf{I}_\ell:\boldsymbol{\beta}_\ell=-\mathbf{I}_\ell:\nabla_\ell\mathbf{p}.\tag{4}$$

In the bulk, at the two nematic-isotropic interfaces, and at the triple line the nematic ordering is defined by the symmetric traceless tensor order parameter [8] $\mathbf{Q}=\mathbf{Q}(\mathbf{x}_p)$, where $\mathbf{x}_p$ is the position vector. The tensor order parameter $\mathbf{Q}$ can be expressed as

$$\mathbf{Q}=r_1\mathbf{nn}+r_2\mathbf{mm}+r_3\mathbf{I}.\tag{5}$$

The orthogonal eigenvectors of $\mathbf{Q}$ appearing in Eq. (2) are known as the director $\mathbf{n}$ and the biaxial director $\mathbf{m}$. The restrictions on $\mathbf{Q}$ are $\mathbf{Q}:\mathbf{I}=0$ and $\mathbf{Q}=\mathbf{Q}^T$, where the superscript T denotes the transpose. The first restriction gives $r_1+r_2+3r_3=0$. Physically significant expressions for these coefficients are

$$r_1=s_1+\frac{s_2}{3},\quad r_2=\frac{2s_2}{3}\quad r_3=-(s_1+s_2)/3,\tag{6}$$

where s_1 and s_2 are the uniaxial scalar order parameter and biaxial scalar order parameter, respectively. For isotropic states $s_1=s_2=0$ $(r_1=r_2=r_3=0)$, while for uniaxial states $s_2=0$ $(r_1=3r_3)$.

B. Bulk, interface, and line nematic elasticity

In this section the bulk, surface, and linear free energies are presented and discussed in reference to interfacial and triple line phenomena. For simplicity and when no ambiguity arises we drop the (i,j) superscripts to refer to the $\Sigma^{(i,j)}$ interface.

Generalizing the Landau–de Gennes theory, the total free energy of the nematic liquid crystal in the region R^1, bounded by S^n, and the triple line C^{tl} is given by

$$F=\int_{R^1}f_b(\mathbf{Q},\nabla\mathbf{Q})dV+\int_{S^n}f_s(\mathbf{Q},\nabla_s\mathbf{Q},\boldsymbol{\xi})dA$$
$$+\int_{c^{\mathrm{tl}}}f_\ell(\mathbf{Q},\nabla_\ell\mathbf{Q},\mathbf{t})d\ell.\tag{7}$$

In this paper we assume that the bulk, interface, and line free energy densities in the Landau–de Gennes model have homogeneous and gradient contributions:

$$f_b(\mathbf{Q},\nabla\mathbf{Q})=f_{bh}(\mathbf{Q})+f_{bg}(\nabla\mathbf{Q}),$$
$$f_s(\mathbf{Q},\nabla_s\mathbf{Q},\boldsymbol{\xi})=f_{sh}(\mathbf{Q},\boldsymbol{\xi})+f_{sg}(\nabla_s\mathbf{Q}),\tag{8a}$$
$$f_\ell(\mathbf{Q},\nabla\mathbf{Q},\mathbf{t})=f_{\ell h}(\mathbf{Q},\mathbf{t})+f_{\ell g}(\nabla_\ell\mathbf{Q}).\tag{8b}$$

The Frank elastic gradient free energy density f_{bg}, the bulk homogeneous free energy density f_{bh}, the interfacial homogeneous free energy density f_{sh}, and the interfacial gradient free energy density f_{sg} are given by [3,4,26]

$$f_{bh}(\mathbf{Q})=a_1\,\mathrm{tr}\,\mathbf{Q}^2-a_2\,\mathrm{tr}\,\mathbf{Q}^3+a_3(\mathrm{tr}\,\mathbf{Q}^2)^2,\tag{9a}$$

$$f_{bg}(\nabla\mathbf{Q})=\frac{L_1}{2}\mathrm{tr}\,\nabla\mathbf{Q}^2+\frac{L_2}{2}(\nabla\cdot\mathbf{Q})\cdot(\nabla\cdot\mathbf{Q})^T,\tag{9b}$$

$$f_{sh}(\mathbf{Q},\boldsymbol{\xi})=f_{s\ \mathrm{iso}}+f_{s\ \mathrm{an}};$$
$$f_{s\ \mathrm{an}}=z_{11}\boldsymbol{\xi}\cdot\mathbf{Q}\cdot\boldsymbol{\xi}+z_{20}\mathbf{Q}:\mathbf{Q}+z_{21}\mathbf{Q}\cdot\boldsymbol{\xi}\cdot\boldsymbol{\xi}\cdot\mathbf{Q}$$
$$+z_{22}(\boldsymbol{\xi}\cdot\mathbf{Q}\cdot\boldsymbol{\xi})^2,\tag{9c}$$

$$f_{sg}=\frac{L_3}{2}\boldsymbol{\xi}\cdot(\mathbf{Q}:\nabla_s\mathbf{Q}-\mathbf{Q}\cdot\nabla_s\cdot\mathbf{Q}),\tag{9d}$$

where ∇ is the gradient operator, $\{L_i\}$, $i=1,2$, are the Frank elastic constants (energy/length), $\{a_i\}$, $i=1,2,3$, are the Landau coefficients (energy/volume), $f_{s\ \mathrm{iso}}$ is the isotropic interfacial tension, $f_{s\ \mathrm{an}}$ is the interfacial anchoring energy, $\{z_{ii}\}$ are the anchoring coefficients (energy/area), and $\boldsymbol{\xi}$ is the unit normal.

The line energies for the generalized Landau–de Gennes model can be written down using the same standard procedures as for the bulk and surface contributions. The homogeneous line free energy density is

$$f_{\ell h}(\mathbf{Q},\mathbf{t}) = f_{\ell\ \mathrm{iso}} + f_{\ell\ \mathrm{an}};$$

$$f_{\ell\ \mathrm{an}} = c_{11}\mathbf{t}\cdot\mathbf{Q}\cdot\mathbf{t} + c_{20}\mathbf{Q}:\mathbf{Q} + c_{21}(\mathbf{Q}\cdot\mathbf{t})\cdot(\mathbf{Q}\cdot\mathbf{t}) + c_{22}(\mathbf{t}\cdot\mathbf{Q}\cdot\mathbf{t})^2, \tag{10}$$

where $f_{\ell\ \mathrm{iso}}$ is the isotropic contribution and $f_{\ell\ \mathrm{an}}$ is the line anchoring energy density. The line gradient free energy density $f_{\ell g}$ is

$$f_{\ell g} = A^1_{ijk}\boldsymbol{\nabla}_{\ell k}Q_{ij} + A^2_{ijklmn}\boldsymbol{\nabla}_{\ell k}Q_{ij}\boldsymbol{\nabla}_{\ell n}Q_{lm}. \tag{11}$$

Using the restrictions $A^1_{ijk} = A^1_{jik}$ and $A^1_{ijk} = A^1_{ij0}I_{\ell 0k}$, then

$$A^1_{ijk}\boldsymbol{\nabla}_{\ell k}Q_{ij} = (\ell_1 t_i t_j t_k + \ell_2 Q_{ij}t_k)\boldsymbol{\nabla}_{\ell k}Q_{ij} \tag{12}$$

where (ℓ_1, ℓ_2) are elastic constants. To find the second order tensor coefficient $\mathbf{A}^2$ we use $A^2_{ijklmn} = A^2_{lmnijk} = A^2_{jiklmn} = A^2_{ijkmln} = A^2_{ijklmn} = A^2_{ij0lmn}I_{\ell 0k} = A^2_{ijklm0}I_{\ell 0k}$, and when using the one-constant approximation its contribution is $A^2_{ijklmn}\boldsymbol{\nabla}_{\ell k}Q_{ij}\boldsymbol{\nabla}_{\ell n}Q_{lm} = \ell_3\boldsymbol{\nabla}_{\ell k}Q_{ij}\boldsymbol{\nabla}_{\ell k}Q_{ij}/2$, where $\ell_3 > 0$ is an elastic coefficient. Thus to lowest order the line energy is

$$f_{\ell g} = \ell_1(\boldsymbol{\nabla}_\ell\cdot\mathbf{Q})\cdot\mathbf{t} + \ell_2\frac{\partial\mathbf{Q}}{\partial s}:\mathbf{Q} + \frac{\ell_3}{2}\boldsymbol{\nabla}_\ell\mathbf{Q}:(\boldsymbol{\nabla}_\ell\mathbf{Q})^T \tag{13}$$

were we used $\mathbf{tt}:(\boldsymbol{\nabla}_\ell\mathbf{Q}) = \boldsymbol{\nabla}_\ell\cdot\mathbf{Q}$, and $(\mathbf{t}\cdot\boldsymbol{\nabla}_\ell)\mathbf{Q} = \partial\mathbf{Q}/\partial s$. It will be shown that the generalized line energy density results in a natural and consistent system of balance equations. In addition, the line stress and torque constitutive equations will be shown to have exact analogs to the corresponding bulk and surface terms.

C. Balance equations for nematic bulk, interface, and triple line phases

To write down the force balance equations we introduce the following stress tensors: the bulk stress tensor $\mathbf{T}_b^{(i)}$ (energy/volume), the interface stress tensor $\mathbf{T}_s^{(i,j)}$ (energy/area), and the triple line stress tensor $\mathbf{T}_\ell$ (energy/length). The dimensionalities of the stress tensors are $\mathbf{T}_b^{(i)}$, 3×3, $\mathbf{t}_s^{(i,j)}$, 2×3, and $\mathbf{T}_\ell$, 1×3. We recall that phases 2 and 3 are isotropic and incapable of sustaining torques. To write down the torque balance equations we introduce the duals $\mathbf{T}_{bx}^{(l)} = -\boldsymbol{\varepsilon}:\mathbf{T}_b^{(l)}$ for the nematic bulk phase, $\mathbf{T}_{sx}^{(i,j)} = -\boldsymbol{\varepsilon}:\mathbf{T}_s^{(i,j)}$ for the two nematic interfaces, and $\mathbf{T}_{\ell x} = -\boldsymbol{\varepsilon}:\mathbf{T}_\ell$ for the triple line. These dual vectors contain the asymmetric information of the stress tensors. In addition we have to take into account the following couple stress tensors: the nematic bulk couple stress tensor $\mathbf{C}_b^{(1)}$ (energy/area), the interface couple stress tensor $\mathbf{C}_s^{(i,j)}$ (energy/length), and the triple line couple stress tensor $\mathbf{C}_\ell$ (energy). The dimensionalities of the couple stress

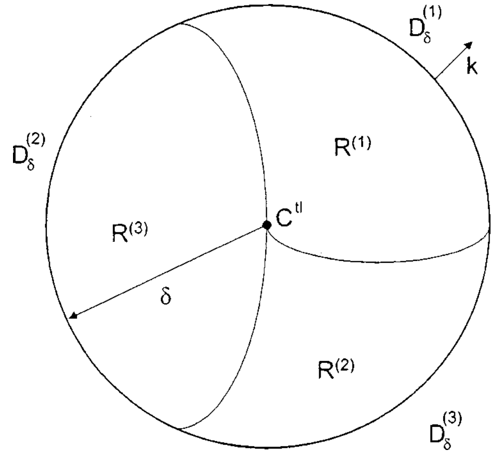

FIG. 2. Schematic of a circular path of radius δ around the triple line C^{tl}. The outward unit normal is $\mathbf{k}$. Calculation of junction integrals to compute long range bulk forces involves integration around C^{cl}.

tensors are $\mathbf{C}_b^{(l)}$, 3×3, $\mathbf{C}_s^{(i,j)}$, 2×3, and $\mathbf{C}_\ell$, 1×3. Due to their dimensionality these tensors obey

$$\mathbf{T}_s^{(i,j)} = \mathbf{I}_s\cdot\mathbf{T}_s^{(i,j)}, \tag{14a}$$

$$\mathbf{T}_\ell = \mathbf{I}_\ell\cdot\mathbf{T}_\ell, \tag{14b}$$

$$\mathbf{C}_s^{(i,j)} = \mathbf{I}_s\cdot\mathbf{C}_s^{(i,j)}, \tag{14c}$$

$$\mathbf{C}_\ell = \mathbf{I}_\ell\cdot\mathbf{C}_\ell. \tag{14d}$$

In addition, we also make use of the following junction integrals:

$$\oint_{\mathrm{jun}}(\mathbf{k}\cdot\mathbf{T}_b)d\ell = \lim_{\delta\to 0}\sum_i \int_{D_\delta^{(i)}}(\mathbf{k}\cdot\mathbf{T}_b^{(i)})d\ell, \tag{15a}$$

$$\oint_{\mathrm{jun}}(\mathbf{k}\cdot\mathbf{C}_b)d\ell = \lim_{\delta\to 0}\int_{D_\delta^{(i)}}(\mathbf{k}\cdot\mathbf{C}_b^{(l)})d\ell, \tag{15b}$$

where $D_\delta^{(i)}$ is the arc of a circle of radius δ lying on phase (i); the center of the circle is the triple line C^{tl} (see Fig. 2). Since the isotropic phases do not support torques, $\mathbf{C}_b^{(2)} = \mathbf{C}_b^{(3)} = \mathbf{0}$, and hence these couples are excluded from Eq. (15b). Bulk long range effects at the triple line vanish when

$$\oint_{\mathrm{jun}}(\mathbf{k}\cdot\mathbf{T}_b)d\ell = 0, \tag{16a}$$

$$\oint_{\mathrm{jun}}(\mathbf{k}\cdot\mathbf{C}_b)d\ell = 0, \tag{16b}$$

which arises whenever $\mathbf{T}_b \approx r^{-\lambda}$, $\mathbf{C}_b \approx r^{-\lambda}$, $\lambda \leqslant 1$, or when $\mathbf{k}\cdot\mathbf{T}_b = 0$, $\mathbf{k}\cdot\mathbf{C}_b = 0$. Junction sums involving interfacial stress and interfacial couples at the contact line are defined by

$$\sum_{\mathrm{jun}} \boldsymbol{\nu}\cdot \mathbf{T}_s = \lim_{\delta\to 0}\sum_{i,j} (\boldsymbol{\nu}^{(i,j)}\cdot \mathbf{T}_s^{(i,j)})|_{c_\delta^{(i,j)}}$$
$$= \boldsymbol{\nu}^{(1,2)}\cdot \mathbf{T}_s^{(1,2)} + \boldsymbol{\nu}^{(3,1)}\cdot \mathbf{T}_s^{(3,1)} + \boldsymbol{\nu}^{(2,3)}\cdot \mathbf{T}_s^{(2,3)}|_{C^{\mathrm{tl}}}, \tag{17a}$$

$$\sum_{\mathrm{jun}} \boldsymbol{\nu}\cdot \mathbf{C}_s = \lim_{\delta\to 0}\sum_{i,j} (\boldsymbol{\nu}^{(i,j)}\cdot \mathbf{C}_s^{(i,j)})|_{e_\delta^{(i,j)}}$$
$$= \boldsymbol{\nu}^{(1,2)}\cdot \mathbf{C}_s^{(1,2)} + \boldsymbol{\nu}^{(3,1)}\cdot \mathbf{C}_s^{(3,1)}|_{C^{\mathrm{tl}}}, \tag{17b}$$

where $e_\delta^{(i,j)}$ are the three intersections of the surface of discontinuities $\Sigma^{(i,j)}$ and the circle D_δ centered on the triple line C^{tl}. Jumps in the bulk stresses $[\boldsymbol{\xi}\cdot \mathbf{T}_b]$ and couple stresses across interfaces are denoted as

$$[\boldsymbol{\xi}\cdot \mathbf{T}_b] = \boldsymbol{\xi}^{(i,j)}\cdot[\mathbf{T}_b^{(i)} - \mathbf{T}_b^{(j)}], \quad (i,j) = (1,2),(3,1),(2,3), \tag{18a}$$

$$[\boldsymbol{\xi}\cdot \mathbf{C}_b] = \boldsymbol{\xi}^{(i,j)}\cdot[\mathbf{C}_b^{(i)} - \mathbf{C}_b^{(i)}], \quad (i,j) = (1,2),(3,1), \tag{18b}$$

$$\mathbf{C}_b^{(2)} = \mathbf{C}_b^{(3)} = \mathbf{0}. \tag{18c}$$

Lastly, we define the bulk [14], interface [13], and line torque vectors as follows:

$$\boldsymbol{\Gamma}_b = \mathbf{T}_{bx} + \boldsymbol{\nabla}\cdot \mathbf{C}_b\,, \tag{19a}$$

$$\boldsymbol{\Gamma}_s = \mathbf{T}_{sx} + \boldsymbol{\nabla}\cdot \mathbf{C}_s\,, \tag{19b}$$

$$\boldsymbol{\Gamma}_\ell = \mathbf{T}_{\ell x} + \boldsymbol{\nabla}\cdot \mathbf{C}_\ell\,. \tag{19c}$$

The force balance on the total volume of the system R is [15]

$$\int_S (\boldsymbol{\nu}\cdot \mathbf{T}_b)dA + \int_C \boldsymbol{\mu}\cdot \mathbf{T}_s d\ell + \boldsymbol{\alpha}\cdot \mathbf{T}_\ell|_{E^{\mathrm{tl}(s)}} + \boldsymbol{\alpha}\cdot \mathbf{T}_\ell|_{E^{\mathrm{tl}(e)}} = 0. \tag{20}$$

Using the divergence theorem in the presence of a surface of discontinuity and a triple line, the surface integral becomes [27]

$$\int_S \boldsymbol{\nu}\cdot \mathbf{T}_b dA = \int_R \boldsymbol{\nabla}\cdot \mathbf{T}_b dV + \int_\Sigma [\boldsymbol{\xi}\cdot \mathbf{T}_b] dA + \int_{C^{\mathrm{il}}}\left(\oint_{\mathrm{jun}} (\mathbf{k}\cdot \mathbf{T}_b) d\ell\right) d\ell. \tag{21}$$

Using the surface divergence theorem the surface stress term becomes [9]

$$\oint_C \boldsymbol{\mu}\cdot \mathbf{T}_s d\ell = \int_\Sigma \boldsymbol{\nabla}_s\cdot \mathbf{T}_s dA + \int_{C^{\mathrm{tl}}}\left(\sum_{\mathrm{jun}} \boldsymbol{\nu}\cdot \mathbf{T}_s\right) d\ell. \tag{22}$$

Using the line divergence theorem the triple line contribution gives [8]

$$\boldsymbol{\alpha}\cdot \mathbf{T}_\ell|_{E^{\mathrm{tl}(s)}} + \boldsymbol{\alpha}\cdot \mathbf{T}_\ell|_{E^{\mathrm{tl}(e)}} = \int_{C^{\mathrm{tl}}} \boldsymbol{\nabla}_\ell\cdot \mathbf{T}_\ell d\ell. \tag{23}$$

Collecting the bulk, interface, and line terms yields the following integral force balances:

$$\int_R \boldsymbol{\nabla}\cdot \mathbf{T}_b dV = 0, \tag{24a}$$

$$\int_\Sigma (\boldsymbol{\nabla}_s\cdot \mathbf{T}^s + [\boldsymbol{\xi}\cdot \mathbf{T}_b]) dA = 0, \tag{24b}$$

$$\int_{C^{\mathrm{tl}}}\left(\boldsymbol{\nabla}_\ell\cdot \mathbf{T}_\ell + \sum_{\mathrm{jun}} \boldsymbol{\nu}\cdot \mathbf{T}_s + \oint_{\mathrm{jun}} (\mathbf{k}\cdot \mathbf{T}_b) d\ell\right) d\ell = 0, \tag{24c}$$

which are satisfied when

$$\boldsymbol{\nabla}\cdot \mathbf{T}_b^{(i)} = 0, \quad i = 1,2,3, \tag{25a}$$

$$\boldsymbol{\nabla}_s\cdot \mathbf{T}_s^{(i,j)} + [\mathbf{k}\cdot \mathbf{T}_b] = 0, \quad (i,j) = (1,2),(3,1),(2,3), \tag{25b}$$

$$\boldsymbol{\nabla}_\ell\cdot \mathbf{T}_\ell + \sum_{\mathrm{jun}} \boldsymbol{\nu}\cdot \mathbf{T}_s + \oint_{\mathrm{jun}} (\mathbf{k}\cdot \mathbf{T}_b) d\ell = 0 \quad \text{on} \quad C^{\mathrm{tl}}. \tag{25c}$$

Thus the complete force balance at the triple line has line, interface, and bulk contributions:

$$\underbrace{\boldsymbol{\nabla}_\ell\cdot \mathbf{T}_\ell}_{\text{line}} + \underbrace{\boldsymbol{\nu}^{(1,2)}\cdot \mathbf{T}_s^{(1,2)} + \boldsymbol{\nu}^{(3,1)}\cdot \mathbf{T}_s^{(3,1)} + \boldsymbol{\nu}^{(2,3)}\cdot \mathbf{T}_s^{(2,3)}|_{C^{\mathrm{tl}}}}_{\text{interface}} + \underbrace{\oint_{\mathrm{jun}} (\mathbf{k}\cdot \mathbf{T}_b) d\ell}_{\text{bulk}} = 0. \tag{26}$$

Bulk, interface, and line long range effects enter in each corresponding term.

In the absence of line energy and long range energy effects the force balance equation (26) simplifies to the well-known classical Neumann equation [8,9]

$$\sum_{\text{jun}} \boldsymbol{\nu}\cdot\mathbf{T}_s = \lim_{\delta\to 0}\sum_{i,j} (\boldsymbol{\nu}^{(i,j)}\cdot\mathbf{T}_s^{(i,j)})|_{e_\delta^{(i,j)}} = \boldsymbol{\nu}^{(1,2)}\cdot\mathbf{T}_s^{(1,2)}+\boldsymbol{\nu}^{(3,1)}\cdot\mathbf{T}_s^{(3,1)}+\boldsymbol{\nu}^{(2,3)}\cdot\mathbf{T}_s^{(2,3)}|_{C^{\text{tl}}} = 0. \tag{27}$$

The torque balance on the nematic region R^1 is

$$\int_{S^1}\mathbf{r}\times(\boldsymbol{\nu}\cdot\mathbf{T}_b)dA+\int_{C^{123}}(\mathbf{r}\times\boldsymbol{\mu}\cdot\mathbf{T}_s)d\ell+\mathbf{r}\times\{\boldsymbol{\alpha}\cdot\mathbf{T}_\ell|_{E^{\text{tl}(s)}}+\boldsymbol{\alpha}\cdot\mathbf{T}_\ell|_{E^{\text{tl}(e)}}\}+\int_{S^1}(\boldsymbol{\nu}\cdot\mathbf{C}_b)dA+\int_{C^{123}}\boldsymbol{\mu}\cdot\mathbf{C}_s d\ell+\{\boldsymbol{\alpha}\cdot\mathbf{C}_\ell|_{E^{\text{tl}(s)}}+\boldsymbol{\alpha}\cdot\mathbf{C}_\ell|_{E^{\text{tl}(e)}}\}=0, \tag{28}$$

where $C^{123}=C^{(1,2)}+C^{(3,1)}$. Next we use the bulk, surface, and line divergence theorem to evaluate the six terms in order of appearence in Eq. (28). Using the divergence theorem on the bulk stress term yields

$$\int_{S^1}\mathbf{r}\times(\boldsymbol{\nu}\cdot\mathbf{T}_b)dA=\int_{R^1}\nabla\cdot(\mathbf{r}\times\mathbf{T}_b)dV+\int_{\Sigma^{123}}\mathbf{r}\times[\mathbf{k}\cdot\mathbf{T}_b]dA+\int_{C^{\text{tl}}}\left(\oint_{\text{jun}}\mathbf{r}\times(\mathbf{k}\cdot\mathbf{T}_b)d\ell\right)d\ell. \tag{29}$$

The first term on the right hand side of Eq. (29) is

$$\nabla\cdot(\mathbf{r}\times\mathbf{T}_b)=\mathbf{r}\times(\nabla\cdot\mathbf{T}_b)+\mathbf{T}_{bx}=+\mathbf{T}_{bx}, \tag{30}$$

where the second equality follows because $\nabla\cdot\mathbf{T}_b=0$. Replacing Eq. (30) into Eq. (29) gives

$$\int_{S^2}\mathbf{r}\times(\boldsymbol{\nu}\cdot\mathbf{T}_b)dA=\int_{R^2}\mathbf{T}_{bx}dV+\int_{\Sigma^{123}}\mathbf{r}\times[\mathbf{k}\cdot\mathbf{T}_b]dA+\int_{C^{\text{tl}}}\left(\oint_{\text{jun}}\mathbf{r}\times(\mathbf{k}\cdot\mathbf{T}_b)d\ell\right)d\ell=0 \tag{31}$$

where $\Sigma^{123}=\Sigma^{(12)}+\Sigma^{(31)}$. Similarly, using the identity

$$\nabla\cdot(\mathbf{r}\times\mathbf{T}_s)=\mathbf{r}\times(\nabla\cdot\mathbf{T}_s)+\mathbf{T}_{sx}=-\mathbf{r}\times[\mathbf{k}\cdot\mathbf{T}_b]+\mathbf{T}_{sx}, \tag{32}$$

the application of the surface divergence theorem gives

$$\oint_{C^{123}}\mathbf{r}\times\boldsymbol{\mu}\cdot\mathbf{T}_s d\ell=\int_{\Sigma^{123}}(-\mathbf{r}\times[\mathbf{k}\cdot\mathbf{T}_b]+\mathbf{T}_{sx})dA+\int_{C^{\text{tl}}}\mathbf{r}\times\left(\sum_{\text{jun}}\boldsymbol{\nu}\cdot\mathbf{T}_s\right)d\ell. \tag{33}$$

Using

$$\nabla\cdot(\mathbf{r}\times\mathbf{T}_\ell)=\mathbf{r}\times(\nabla\cdot\mathbf{T}_\ell)+\mathbf{T}_{\ell x} = -\mathbf{r}\times\left(\sum_{\text{jun}}\boldsymbol{\nu}\cdot\mathbf{t}_s+\oint_{\text{jun}}(\mathbf{k}\cdot\mathbf{T}_b)d\ell\right)+\mathbf{T}_{\ell x} \tag{34}$$

and the line divergence theorem, the torque from the linear stress becomes

$$\mathbf{r}\times\{\mathbf{x}\cdot\mathbf{T}_\ell|_{E^{\text{tl}(s)}}+\boldsymbol{\alpha}\cdot\mathbf{T}_\ell|_{E^{\text{tl}(c)}}\} =\int_{C^{\text{tl}}}\nabla_\ell\cdot(\mathbf{r}\times\mathbf{T}_\ell)d\ell =\int_{C^{\text{tl}}}\left\{-\mathbf{r}\times\left(\sum_{\text{jun}}\boldsymbol{\nu}\cdot\mathbf{T}_s+\oint_{\text{jun}}(\mathbf{k}\cdot\mathbf{T}_b)d\ell\right)+\mathbf{T}_{\ell x}\right\}d\ell. \tag{35}$$

We now proceed with the bulk, surface, and line couple stresses, and obtain

$$\int_{S^2}\boldsymbol{\nu}\cdot\mathbf{C}_b dA=\int_{R^2}\nabla\cdot\mathbf{C}_b dV+\int_{\Sigma^{123}}[\boldsymbol{\xi}\cdot\mathbf{C}_b]dA+\int_{C^{\text{tl}}}\left(\oint_{\text{jun}}(\mathbf{k}\cdot\mathbf{C}_b)d\ell\right)d\ell, \tag{36a}$$

$$\oint_{C^{123}}\boldsymbol{\mu}\cdot\mathbf{C}_s d\ell=\int_{\Sigma^{123}}\nabla_s\cdot\mathbf{C}_s dA+\int_{C^{\text{tl}}}\left(\sum_{\text{jun}}\boldsymbol{\nu}\cdot\mathbf{C}_s\right)d\ell, \tag{36b}$$

$$\boldsymbol{\alpha}\cdot\mathbf{C}_\ell|_{E^{\text{tl}(s)}}+\boldsymbol{\alpha}\cdot\mathbf{C}_\ell|_{E^{\text{tl}(e)}}=\int_{C^{\text{tl}}}\nabla_\ell\cdot\mathbf{C}_\ell d\ell. \tag{36c}$$

Collecting terms we find the bulk, interface, and line balances for the nematic phase:

$$\int_{R^1}\{\mathbf{T}_{bx}+\nabla\cdot\mathbf{C}_b\}dV=0, \tag{37a}$$

$$\int_{\Sigma^{123}}\{\mathbf{T}_{sx}+\nabla_s\cdot\mathbf{C}_s+[\boldsymbol{\xi}\cdot\mathbf{C}_b]\}dA=0, \tag{37b}$$

$$\int_{C^{\text{tl}}}\left\{\mathbf{T}_{\ell x}+\nabla_\ell\cdot\mathbf{C}_\ell+\left(\sum_{\text{jun}}\boldsymbol{\nu}\cdot\mathbf{C}_s\right)+\oint_{\text{jun}}(\mathbf{k}\cdot\mathbf{C}_b)d\ell\right\}d\ell=0. \tag{37c}$$

Thus the differential torque balances on the nematic bulk, interfaces, and line phases are

$$\mathbf{T}_{bx}^{(1)}+\nabla\cdot\mathbf{C}_b^{(1)}=0, \tag{38a}$$

$$\mathbf{T}_{sx}^{(i,j)}+\nabla_s\cdot\mathbf{C}_s^{(i,j)}+[\boldsymbol{\xi}\cdot\mathbf{C}_b]=0,\quad (i,j)=(1,2),(3,1), \tag{38b}$$

$$\mathbf{T}_{\ell x}+\nabla_\ell\cdot\mathbf{C}_\ell+\left(\sum_{\text{jun}}\boldsymbol{\nu}\cdot\mathbf{C}_s\right)+\oint_{\text{jun}}(\mathbf{k}\cdot\mathbf{C}_b)d\ell=0,\quad \text{on } C^{\text{tl}}. \tag{38c}$$

"In terms of torque vectors the balance equations read

$$\boldsymbol{\Gamma}_b^{(1)}=0 \tag{39a}$$

$$\boldsymbol{\Gamma}_s^{(i,j)}+[\boldsymbol{\xi}\cdot\mathbf{C}_b]=0,\quad (i,j)=(1,2),(3,1), \tag{39b}$$

$$\boldsymbol{\Gamma}_\ell+\left(\sum_{\text{jun}}\boldsymbol{\nu}\cdot\mathbf{C}_s\right)+\oint_{\text{jun}}(\mathbf{k}\cdot\mathbf{C}_b)d\ell=0. \tag{39c}$$

The torque balance equation at the triple line has the following line, surface, and bulk contributions:

$$\underbrace{\mathbf{T}_{\ell x}+\boldsymbol{\nabla}_\ell\cdot\mathbf{C}_\ell}_{\text{line}}+\underbrace{\left(\sum_{\text{jun}}\boldsymbol{\nu}\cdot\mathbf{C}_s\right)}_{\text{interface}}+\underbrace{\oint_{\text{jun}}(\mathbf{k}\cdot\mathbf{C}_b)d\ell}_{\text{bulk}}=0. \tag{40}$$

Bulk, interface, and line long range effects enter in each corresponding term. In the absence of line energy and long range bulk contributions the torque balance equation reduces to the analog of the Neumann force balance equation:

$$\sum_{\text{jun}}\boldsymbol{\nu}\cdot\mathbf{C}_s=0. \tag{41}$$

D. Constitutive equations for bulk, surface, and line stresses, couple stresses, and torques

The force and torque balance equations at triple lines require constitutive equations for $\mathbf{T}_b$, $\mathbf{T}_s$, $\mathbf{T}_\ell$, $\mathbf{C}_b$, $\mathbf{C}_s$, $\mathbf{C}_\ell$, $\boldsymbol{\Gamma}_b$, $\boldsymbol{\Gamma}_s$, and $\boldsymbol{\Gamma}_\ell$, in their corresponding isotropic and nematic bulk, interface, and line phases. The bulk stresses and interfacial stresses for the isotropic fluids are

$$\mathbf{T}_b^{(i)}=-p^{(i)}\mathbf{I},\quad i=2,3, \tag{42a}$$

$$\mathbf{T}_s^{(2,3)}=f_{\text{sh}}^{(2,3)}\mathbf{I}_s, \tag{42b}$$

where $p^{(i)}$ is the pressure and $f_{sh}^{(2,3)}$ is the interfacial tension. The constitutive equations for bulk and interfacial stresses and torques in the Landau–de Gennes model involving the nematic phase have been presented previously (see, for example, [3,10,13]). The constitutive equations are as follows.

(a) Bulk stress tensor, bulk couple stress tensor, and bulk torque vector

$$\mathbf{T}_b^{(1)}=-(p^{(1)}-f_b)\mathbf{I}-\frac{\partial f_b}{\partial\boldsymbol{\nabla}\mathbf{Q}}:(\boldsymbol{\nabla}\cdot\mathbf{Q})^T, \tag{43a}$$

$$\mathbf{C}_b^{(1)}=\left\{\left[\frac{\partial f_b}{\partial\boldsymbol{\nabla}\mathbf{Q}}+\left(\frac{\partial f_b}{\partial\boldsymbol{\nabla}\mathbf{Q}}\right)^T\right]\cdot\mathbf{Q}\right\}:\boldsymbol{\varepsilon}, \tag{43b}$$

$$C_{b0k}=\left(\frac{\partial f}{\partial\boldsymbol{\nabla}_0 Q_{il}}+\left(\frac{\partial f}{\partial\boldsymbol{\nabla}_0 Q_{li}}\right)^T\right)Q_{lj}\varepsilon_{jik}, \tag{43c}$$

$$\boldsymbol{\Gamma}_b^{(1)}=\mathbf{t}_{bx}^{(1)}+\boldsymbol{\nabla}\cdot\mathbf{C}_b^{(1)}=\boldsymbol{\varepsilon}:\left(\frac{\partial f_b}{\partial\boldsymbol{\nabla}\mathbf{Q}}:(\boldsymbol{\nabla}\cdot\mathbf{Q})^T\right)+\boldsymbol{\nabla}\cdot\left(\left\{\left[\frac{\partial f_b}{\partial\boldsymbol{\nabla}\mathbf{Q}}+\left(\frac{\partial f_b}{\partial\boldsymbol{\nabla}\mathbf{Q}}\right)^T\right]\cdot\mathbf{Q}\right\}:\boldsymbol{\varepsilon}\right) \tag{43d}$$

where $(\mathbf{A}^T)_{ijk}=\mathbf{A}_{ikj}$ [13].

(b) Surface stress tensor, surface couple stress tensor, and surface torque vector

For the Eqs. (13) and (12) nematic interfaces, the surface stress tensor is [13]

$$\mathbf{T}_s=\mathbf{T}_{sn}+\mathbf{T}_{sd}+\mathbf{T}_{sb} \tag{44}$$

where the normal $\mathbf{T}_{sn}$, distortion $\mathbf{T}_{sd}$, and bending $\mathbf{T}_{sb}$ components are

$$\mathbf{T}_{sn}(\mathbf{Q},\boldsymbol{\xi}^{(i,j)},\boldsymbol{\nabla}_s\mathbf{Q})=f_s^{(i,j)}\mathbf{I}_s,\quad (i,j)=(1,2),(3,1), \tag{45a}$$

$$\mathbf{T}_{sd}^{(i,j)}(\mathbf{Q},\xi^{(i,j)},\boldsymbol{\nabla}_s\mathbf{Q})=-\frac{\partial f_s^{(i,j)}}{\partial\boldsymbol{\nabla}_s\mathbf{Q}}:(\boldsymbol{\nabla}_s\mathbf{Q})^{\mathrm{T}},\quad (i,j)=(1,2),(3,1) \tag{45b}$$

$$\mathbf{T}_{sb}^{(i,j)}(\mathbf{Q},\boldsymbol{\xi}^{(i,j)},\boldsymbol{\nabla}_s\mathbf{Q})=-\mathbf{I}_s\cdot\frac{\partial f_s^{(i,j)}}{\partial\boldsymbol{\xi}^{(i,j)}}\xi^{(i,j)},\quad (i,j)=(1,2),(3,1) \tag{45c}$$

$$\mathbf{C}_s^{(i,j)}=\left\{\left[\frac{\partial f_s^{(i,j)}}{\partial\boldsymbol{\nabla}_s\mathbf{Q}}+\left(\frac{\partial f_s^{(i,j)}}{\partial\boldsymbol{\nabla}_s\mathbf{Q}}\right)^T\right]\cdot\mathbf{Q}\right\}:\boldsymbol{\varepsilon},\quad (i,j)=(1,2),(3,1), \tag{45d}$$

$$\begin{aligned}\boldsymbol{\Gamma}_s^{(i,j)}&=\mathbf{t}_{sx}^{(i,j)}+\boldsymbol{\nabla}\cdot\mathbf{C}_s^{(i,j)}\\&=\boldsymbol{\varepsilon}:\left[\mathbf{I}_s\cdot\left(\frac{\partial f_s^{(i,j)}}{\partial\boldsymbol{\xi}^{(i,j)}}\boldsymbol{\xi}^{(i,j)}\right)+\frac{\partial f_s^{(i,j)}}{\partial\boldsymbol{\nabla}_s\mathbf{Q}}:(\boldsymbol{\nabla}_s\mathbf{Q})^T\right]\\&\quad+\boldsymbol{\nabla}_s\cdot\left(\left\{\left[\frac{\partial f_s^{(i,j)}}{\partial\boldsymbol{\nabla}_s\mathbf{Q}}+\left(\frac{\partial f_s^{(i,j)}}{\partial\boldsymbol{\nabla}_s\mathbf{Q}}\right)^T\right]\cdot\mathbf{Q}\right\}:\boldsymbol{\varepsilon}\right),\\&\quad (i,j)=(1,2),(3,1).\end{aligned} \tag{45e}$$

(c) Line stress tensor, line couple stress tensor, and line torque vector

In this section we present the derivation of line stress tensor, line couple stress tensor, and line torque. With the adopted generalized line free energy $f_\ell=f_\ell(\mathbf{Q},\boldsymbol{\nabla}_\ell\mathbf{Q},\mathbf{t})$, we find that the line stress tensor contains the following normal $\mathbf{T}_{\ell n}$, distortion $\mathbf{T}_{\ell d}$, and bending $\mathbf{T}_{\ell b}$ components:

$$\mathbf{T}_\ell=\mathbf{T}_{\ell n}+\mathbf{T}_{\ell d}+\mathbf{T}_{\ell b}. \tag{46}$$

If the line energy is independent of $\boldsymbol{\nabla}_\ell\mathbf{Q}$ $[f_\ell=f_\ell(\mathbf{Q},\mathbf{t})]$ then there are no distortion stresses. If the line energy has no anchoring contribution then there are no bending stresses. Here we wish to treat the most general and admissible case.

The normal stress components, equivalent to pressure in $\mathbf{T}_b$ and surface tension in $\mathbf{T}_s$, account for the line tension [8]:

$$\mathbf{T}_{\mathrm{ln}} = +f_\ell \mathbf{I}_{\ell\ell}. \tag{47}$$

The distortion stress components, equivalent to bulk Ericksen stress [13], are found from a variation of $\boldsymbol{\nabla}_\ell \mathbf{Q}$ at constant $\mathbf{Q}$ and $\mathbf{t}$:

$$\delta F_\ell = \int_{C^{\mathrm{tl}}} \left(\frac{\partial f_\ell}{\partial \boldsymbol{\nabla}_\ell \mathbf{Q}} \right) \vdots \delta(\boldsymbol{\nabla}_\ell \mathbf{Q})^T d\ell = \int_{C^{\mathrm{tl}}} \mathbf{T}_{\ell d} : (\boldsymbol{\nabla}_\ell \mathbf{u})^T d\ell$$
$$= \int_{C^{\mathrm{tl}}} (\mathbf{I}_\ell \cdot \mathbf{T}_{\ell d}) : (\boldsymbol{\nabla}_\ell \mathbf{u})^T d\ell = \int_{C^{\mathrm{tl}}} (\mathbf{T}_{\ell d} \cdot \mathbf{I}_\ell) : (\boldsymbol{\nabla}_\ell \mathbf{u})^T d\ell, \tag{48}$$

where $\mathbf{u}$ is the displacement, which displaces a point from position $\mathbf{r}$ to $\mathbf{r}'$: $\mathbf{r}' = \mathbf{r} + \mathbf{u}$. Since $\mathbf{Q}'(\mathbf{r}', \mathbf{t}') = \mathbf{Q}(\mathbf{r}, \mathbf{t}')$, differentiation with respect to $\mathbf{r}'$ at constant $\mathbf{t}'$ gives

$$\delta(\boldsymbol{\nabla}_\ell \mathbf{Q})^T = -(\boldsymbol{\nabla}_\ell \mathbf{Q})^T \cdot (\boldsymbol{\nabla}_\ell \mathbf{u})^T \tag{49}$$

and the corresponding distortion stress is

$$\mathbf{T}_{\ell d} = -\frac{\partial f_\ell}{\partial(\boldsymbol{\nabla}_\ell \mathbf{Q})} : (\boldsymbol{\nabla}_\ell \mathbf{Q})^T = \mathbf{I}_\ell \cdot \left(-\frac{\partial f_\ell}{\partial(\boldsymbol{\nabla}_\ell \mathbf{Q})} : (\boldsymbol{\nabla}_\ell \mathbf{Q})^T \right)$$
$$= \left(-\frac{\partial f_\ell}{\partial(\boldsymbol{\nabla}_\ell \mathbf{Q})} : (\boldsymbol{\nabla}_\ell \mathbf{Q})^T \right) \cdot \mathbf{I}_\ell. \tag{50}$$

The distortion stress is a normal stress, $\mathbf{T}_{\ell d} = (\mathbf{I}_\ell : \mathbf{T}_{\ell d}) \mathbf{I}_\ell$, and accounts for tension due to order parameter gradients. The bending contribution is found from a variation due to small changes in the unit tangent vector $\mathbf{t}$:

$$\delta F_\ell = \int_{C^{\mathrm{tl}}} \left(\frac{\partial f_\ell}{\partial \mathbf{t}} \right) \cdot \delta \mathbf{t}\, d\ell = \int_{C^{\mathrm{tl}}} \mathbf{T}_{\ell b} : (\boldsymbol{\nabla}_\ell \mathbf{u})^T d\ell$$
$$= \int_{C^{\mathrm{tl}}} (\mathbf{I}_\ell \cdot \mathbf{T}_{\ell b}) : (\boldsymbol{\nabla}_\ell \mathbf{u})^T d\ell. \tag{51}$$

Next we present the nontrivial derivation of $\delta\mathbf{t}$. To compute $\delta\mathbf{t}$ we introduce a small displacement $\mathbf{u}$ that moves $\mathbf{r}$ to $\mathbf{r}'$: $\mathbf{r}' = \mathbf{r} + \mathbf{u}$. The differential $d\mathbf{r}'$ is

$$d\mathbf{r}' = d\mathbf{r} + d\mathbf{u}. \tag{52}$$

Using the definitions of arclengths $ds'^2 = d\mathbf{r}' \cdot d\mathbf{r}'$ and $ds^2 = d\mathbf{r} \cdot d\mathbf{r}$, the expression for differential arclengths ds' is

$$ds'^2 = ds^2 + 2 d\mathbf{r} \cdot d\mathbf{u}, \tag{53a}$$

$$ds' = ds \left(1 + \frac{d\mathbf{r}}{ds} \cdot \frac{d\mathbf{u}}{ds} \right), \tag{53b}$$

$$e = \frac{ds' - ds}{ds} = \frac{d\mathbf{r}}{ds} \cdot \frac{d\mathbf{u}}{ds} = \mathbf{t} \cdot \frac{d\mathbf{u}}{ds}, \tag{53c}$$

where the symbol e is known as the extension. Since

$$\frac{d\mathbf{u}}{ds} = \left(\frac{\partial \mathbf{u}}{d\mathbf{r}} \right)^T \cdot \left(\frac{d\mathbf{r}}{ds} \right) = (\boldsymbol{\nabla} \mathbf{u})^T \cdot \mathbf{t} = \mathbf{t} \cdot (\boldsymbol{\nabla}_\ell \mathbf{u}), \tag{54}$$

the extension e simplifies to

$$e = \frac{ds' - ds}{ds} = \frac{ds'}{ds} - 1 = \mathbf{tt} : (\boldsymbol{\nabla}_\ell \mathbf{u}), \tag{55}$$

from which we can obtain the following equation for ds/ds':

$$\frac{ds}{ds'} = \frac{1}{1+e} = 1 - \mathbf{tt} : (\boldsymbol{\nabla} \mathbf{u}) = 1 - \mathbf{tt} : (\boldsymbol{\nabla}_\ell \mathbf{u}). \tag{56}$$

Differentiating $\mathbf{r}' = \mathbf{r} + \mathbf{u}$ with respect to $\mathbf{s}'$ we find the relation between $\mathbf{t}$ and $\mathbf{t}'$:

$$\frac{d\mathbf{r}'}{ds'} \equiv \mathbf{t}' = \frac{d\mathbf{r}}{ds} \frac{ds}{ds'} + \frac{d\mathbf{u}}{ds} = \mathbf{t}[1 - \mathbf{tt} : (\boldsymbol{\nabla}_\ell \mathbf{u})] + \mathbf{t} \cdot \boldsymbol{\nabla}_\ell \mathbf{u}$$
$$= \mathbf{t} + (\mathbf{I} + \mathbf{tt}) \mathbf{t} \cdot (\boldsymbol{\nabla}_\ell \mathbf{u}). \tag{57}$$

Thus the small change in the tangent vector $\mathbf{t}$ and the change in line energy due to displacement $\mathbf{u}$ are given by

$$\delta \mathbf{t} = \mathbf{t}' - \mathbf{t} = (\mathbf{I} - \mathbf{tt}) \mathbf{t} \cdot (\boldsymbol{\nabla}_\ell \mathbf{u}), \tag{58a}$$

$$\delta F_\ell = \int_{C^{\mathrm{tl}}} \left(\frac{\partial f_\ell}{\partial \mathbf{t}} \right) \cdot \delta \mathbf{t}\, d\ell = \int_{C^{\mathrm{tl}}} \mathbf{T}_{\ell b} : (\boldsymbol{\nabla}_\ell \mathbf{u})^T d\ell$$
$$= \int_{C^{\mathrm{tl}}} (\mathbf{I}_\ell \cdot \mathbf{T}_{\ell b}) : (\boldsymbol{\nabla}_\ell \mathbf{u})^T d\ell. \tag{58b}$$

From this last result we find that the line bending stress tensor is

$$\mathbf{T}_{\ell b} = \mathbf{t}(\mathbf{I} - \mathbf{tt}) \cdot \frac{\partial f_\ell}{\partial \mathbf{t}} = \mathbf{t}(\mathbf{pp} + \mathbf{bb}) \cdot \frac{\partial f_\ell}{\partial \mathbf{t}}. \tag{59}$$

In the principal line frame $(\mathbf{t}, \mathbf{p}, \mathbf{b})$ the bending stress $\mathbf{T}_{\ell b}$ has two components:

$$\mathbf{T}_{\ell b} = \left(\mathbf{p} \cdot \frac{\partial f_\ell}{\partial \mathbf{t}} \right) \mathbf{tp} + \left(\mathbf{b} \cdot \frac{\partial f_\ell}{\partial \mathbf{t}} \right) \mathbf{tb}. \tag{60}$$

The bending stress takes its name because it only has (**tp**) and (**tb**) components. Collecting results, the total 1×3 line stress tensor is given by

$$\mathbf{T}_\ell = f_\ell \mathbf{I}_s - \frac{\partial f_\ell}{\partial(\boldsymbol{\nabla}_\ell \mathbf{Q})} : (\boldsymbol{\nabla}_\ell \mathbf{Q})^T + \left(\mathbf{p} \cdot \frac{\partial f_\ell}{\partial \mathbf{t}} \right) \mathbf{tp} + \left(\mathbf{b} \cdot \frac{\partial f_\ell}{\partial \mathbf{t}} \right) \mathbf{tb}, \tag{61}$$

which in component form is

$$\mathbf{T}_{\ell b} = T_{\ell b}^{tt} \mathbf{tt} + T_{\ell b}^{tp} \mathbf{tp} + T_{\ell b}^{tb} \mathbf{tb}, \tag{62a}$$

$$T_{\ell b}^{tt}=f_\ell-\mathbf{tt}:\frac{\partial f_\ell}{\partial(\boldsymbol{\nabla}_\ell\mathbf{Q})}:(\boldsymbol{\nabla}_\ell\mathbf{Q})^T,\quad T_{\ell b}^{tp}=\mathbf{p}\cdot\frac{\partial f_\ell}{\partial\mathbf{t}},$$

$$T_{\ell b}^{tb}=\mathbf{b}\cdot\frac{\partial f_\ell}{\partial\mathbf{t}}. \tag{62b}$$

The derivation of the line couple stress tensor is analogous to those of its bulk and surface counterparts and its expression has the same form as theirs:

$$\mathbf{C}_\ell=\left\{\left[\frac{\partial f_\ell}{\partial\boldsymbol{\nabla}_\ell\mathbf{Q}}+\left(\frac{\partial f_\ell}{\partial\boldsymbol{\nabla}_\ell\mathbf{Q}}\right)^{T_{132}}\right]\cdot\mathbf{Q}\right\}:\varepsilon. \tag{63}$$

In the principal line frame the line couple stress tensor $\mathbf{C}_\ell$ becomes

$$\mathbf{C}_\ell=C_\ell^{tt}\mathbf{tt}+C_\ell^{tp}\mathbf{tp}+C_\ell^{tb}\mathbf{tb},\quad C_\ell^{tt}=\mathbf{tt}:\mathbf{C}_\ell,$$

$$C_\ell^{tp}=\mathbf{pt}:\mathbf{C}_\ell,\quad C_\ell^{tb}=\mathbf{bt}:\mathbf{C}_\ell. \tag{64}$$

Next we compute the line torque $\boldsymbol{\Gamma}_\ell$. To derive the dual of the line stress tensor $\mathbf{T}_{\ell x}$ we use its formal definition and get

$$\mathbf{T}_{\ell x}=-\boldsymbol{\varepsilon}:\mathbf{T}_\ell=\mathbf{T}_{\ell bx}=\left(\mathbf{p}\cdot\frac{\partial f_\ell}{\partial\mathbf{t}}\right)\mathbf{b}-\left(\mathbf{b}\cdot\frac{\partial f_\ell}{\partial\mathbf{t}}\right)\mathbf{p}. \tag{65}$$

Thus the line torque vector $\boldsymbol{\Gamma}_\ell$ is given by

$$\boldsymbol{\Gamma}_\ell=\left(\mathbf{p}\cdot\frac{\partial f_\ell}{\partial\mathbf{t}}\right)\mathbf{b}-\left(\mathbf{b}\cdot\frac{\partial f_\ell}{d\mathbf{t}}\right)\mathbf{p}+\boldsymbol{\nabla}_\ell\cdot(C_\ell^{tt}\mathbf{tt}+C_\ell^{tp}\mathbf{tp}+C_\ell^{tb}\mathbf{tb}). \tag{66}$$

Using the Frenet-Serret formulas the line torque simplifies to

$$\boldsymbol{\Gamma}_\ell=\left(\frac{\partial C_\ell^{tt}}{\partial s}-\kappa C_\ell^{tp}\right)\mathbf{t}+\left(-\mathbf{b}\cdot\frac{\partial f_\ell}{\partial\mathbf{t}}+\frac{\partial C_\ell^{tp}}{\partial s}+\kappa C_\ell^{tt}-\tau C_\ell^{tb}\right)\mathbf{p}$$
$$+\left(\mathbf{p}\cdot\frac{\partial f_\ell}{\partial\mathbf{t}}+\frac{\partial C_\ell^{tb}}{\partial s}+\tau C_\ell^{tp}\right)\mathbf{b}, \tag{67}$$

where the contributions of the line anchoring and gradient energies are made clear.

III. BALANCE EQUATIONS FOR NEMATIC TRIPLE LINE PHASES

More tractable expressions of the force and torque balance equations are found by projecting them along the principal ($\mathbf{t}$,$\mathbf{b}$,$\mathbf{p}$) frame. Projecting the line force balance along the principal line frame ($\mathbf{t}$,$\mathbf{p}$,$\mathbf{b}$), we obtain

$$\left(\frac{\partial T_\ell^{tt}}{\partial s}-\kappa T_\ell^{tp}\right)+\mathbf{t}\cdot\left(\sum_{\text{jun}}\boldsymbol{\nu}\cdot\mathbf{T}_s\right)+\mathbf{t}\cdot\left(\oint_{\text{jun}}(\mathbf{k}\cdot\mathbf{T}_b)d\ell\right)=0, \tag{68a}$$

$$\left(\frac{\partial T_\ell^{tp}}{\partial s}+\varkappa T_\ell^{tt}-\tau T_\ell^{tb}\right)+\mathbf{p}\cdot\left(\sum_{\text{jun}}\boldsymbol{\nu}\cdot\mathbf{T}_s\right)+\mathbf{p}\cdot\left(\oint_{\text{jun}}(\mathbf{k}\cdot\mathbf{T}_b)d\ell\right)$$
$$=0, \tag{68b}$$

$$\left(\frac{\partial T_\ell^{tb}}{\partial s}+\tau T_\ell^{tb}\right)+\mathbf{b}\cdot\left(\sum_{\text{jun}}\boldsymbol{\nu}\cdot\mathbf{T}_s\right)+\mathbf{p}\cdot\left(\oint_{\text{jun}}(\mathbf{k}\cdot\mathbf{T}_b)d\ell\right)=0, \tag{68c}$$

Likewise the components of the line torque balance equation are

$$\left(\frac{\partial C_\ell^{tt}}{\partial s}+\kappa C_\ell^{tp}\right)+\mathbf{b}\cdot\left(\sum_{\text{jun}}\boldsymbol{\nu}\cdot\mathbf{C}_s\right)+\mathbf{t}\cdot\left(\oint_{\text{jun}}(\mathbf{k}\cdot\mathbf{C}_b)d\ell\right)=0, \tag{69a}$$

$$\left(-\mathbf{b}\cdot\frac{\partial f_\ell}{\partial\mathbf{t}}+\frac{\partial C_\ell^{tp}}{\partial s}+\varkappa C_\ell^{tt}-\tau C_\ell^{tb}\right)+\mathbf{p}\cdot\left(\sum_{\text{jun}}\boldsymbol{\nu}\cdot\mathbf{C}_s\right)$$
$$+\mathbf{p}\cdot\left(\oint_{\text{jun}}(\mathbf{k}\cdot\mathbf{C}_b)d\ell\right)=0, \tag{69b}$$

$$\left(-\mathbf{p}\cdot\frac{\partial f_\ell}{\partial\mathbf{t}}+\frac{\partial C_\ell^{tb}}{\partial s}+\tau C_\ell^{tp}\right)+\mathbf{b}\cdot\left(\sum_{\text{jun}}\boldsymbol{\nu}\cdot\mathbf{C}_s\right)$$
$$+\mathbf{b}\cdot\left(\oint_{\text{jun}}(\mathbf{k}\cdot\mathbf{C}_b)d\ell\right)=0. \tag{69c}$$

A number of limiting cases worth enumerating arise when certain energies are negligible, and when certain geometric conditions prevail. Below we use the term ''isotropic energy'' to denote negligible anchoring and gradient energy.

(a) Isotropic line energy

$$\frac{\partial f_{\ell h}}{\partial s}+\mathbf{t}\cdot\left(\sum_{\text{jun}}\boldsymbol{\nu}\cdot\mathbf{T}_s\right)+\mathbf{t}\cdot\left(\oint_{\text{jun}}(\mathbf{k}\cdot\mathbf{T}_b)d\ell\right)=0, \tag{70a}$$

$$(f_{\ell h}\kappa)+\mathbf{p}\cdot\left(\sum_{\text{jun}}\boldsymbol{\nu}\cdot\mathbf{T}_s\right)+\mathbf{p}\cdot\left(\oint_{\text{jun}}(\mathbf{k}\cdot\mathbf{T}_b)d\ell\right)=0, \tag{70b}$$

$$\mathbf{b}\cdot\left(\sum_{\text{jun}}\boldsymbol{\nu}\cdot\mathbf{T}_s\right)+\mathbf{b}\cdot\left(\oint_{\text{jun}}(\mathbf{k}\cdot\mathbf{T}_b)d\ell\right)=0, \tag{70c}$$

$$\mathbf{t}\cdot\left(\sum_{\text{jun}}\boldsymbol{\nu}\cdot\mathbf{C}_s\right)+\mathbf{t}\cdot\left(\oint_{\text{jun}}(\mathbf{k}\cdot\mathbf{T}_b)d\ell\right)=0, \tag{70d}$$

$$\mathbf{p}\cdot\left(\sum_{\text{jun}}\boldsymbol{\nu}\cdot\mathbf{C}_s\right)+\mathbf{p}\cdot\left(\oint_{\text{jun}}(\mathbf{k}\cdot\mathbf{C}_b)d\ell\right)=0, \tag{70e}$$

$$\mathbf{b}\cdot\left(\sum_{\text{jun}}\boldsymbol{\nu}\cdot\mathbf{C}_s\right)+\mathbf{b}\cdot\left(\oint_{\text{jun}}(\mathbf{k}\cdot\mathbf{C}_b)d\ell\right)=0. \tag{70f}$$

In this case all balances at the triple line involve surface and bulk components.

(b) Isotropic line and interfacial energies

$$\frac{\partial f_{\ell h}}{\partial s}+\mathbf{t}\cdot\left(\oint_{\text{jun}}(\mathbf{k}\cdot\mathbf{T}_b)d\ell\right)=0, \tag{71a}$$

$$(\varkappa\varkappa f_{\ell h})+\mathbf{p}\cdot\Bigg(\boldsymbol{\nu}^{(1,2)}f_{sh}^{(1,2)}+\boldsymbol{\nu}^{(3,1)}f_{sh}^{(3,1)}+\boldsymbol{\nu}^{(2,3)}f_{sh}^{(2,3)}|_{C^{\mathrm{tl}}} + \oint_{\mathrm{jun}}(\mathbf{k}\cdot\mathbf{T}_b)d\ell\Bigg)=0, \tag{71b}$$

$$\mathbf{b}\cdot\Bigg(\boldsymbol{\nu}^{(1,2)}f_{sh}^{(1,2)}+\boldsymbol{\nu}^{(3,1)}f_{sh}^{(3,1)}+\boldsymbol{\nu}^{(2,3)}f_{sh}^{(2,3)}|_{C^{\mathrm{tl}}}+\oint_{\mathrm{jun}}(\mathbf{k}\cdot\mathbf{T}_b)d\ell\Bigg)=0, \tag{71c}$$

$$\oint_{\mathrm{jun}}(\mathbf{k}\cdot\mathbf{C}_b)d\ell=0. \tag{71d}$$

Equation (71a) is the lineal Marangoni force balance and Eq. (71d) is the vanishing bulk couple condition. No torques act on the triple line. Bulk contributions arise on all balances.

(b) Rectilinear triple lines with constant isotropic line and interfacial energies. Let $(\mathbf{t},\mathbf{p},\mathbf{b})$ represent an orthogonal frame, with $\mathbf{t}$ along the triple line. Then

$$\mathbf{t}\cdot\Bigg(\oint_{\mathrm{jun}}(\mathbf{k}\cdot\mathbf{T}_b)d\ell\Bigg)=0, \tag{72a}$$

$$\mathbf{p}\cdot\Bigg(\boldsymbol{\nu}^{(1,2)}f_{sh}^{(1,2)}+\boldsymbol{\nu}^{(3,1)}f_{sh}^{(3,1)}+\boldsymbol{\nu}^{(2,3)}f_{sh}^{(2,3)}|_{C^{\mathrm{tl}}}+\oint_{\mathrm{jun}}(\mathbf{k}\cdot\mathbf{T}_b)d\ell\Bigg)=0, \tag{72b}$$

$$\mathbf{b}\cdot\Bigg(\boldsymbol{\nu}^{(1,2)}f_{sh}^{(1,2)}+\boldsymbol{\nu}^{(3,1)}f_{sh}^{(3,1)}+\boldsymbol{\nu}^{(2,3)}f_{sh}^{(2,3)}|_{C^{\mathrm{tl}}}+\oint_{\mathrm{jun}}(\mathbf{k}\cdot\mathbf{T}_b)d\ell\Bigg)=0, \tag{72c}$$

$$\oint_{\mathrm{jun}}(\mathbf{k}\cdot\mathbf{C}_b)d\ell=0. \tag{72d}$$

In this case no torques and no tangential forces act on the triple line.

IV. APPLICATIONS

Obviously the balance equations at the triple line are complex and full rigorous solutions to specific problems are beyond the scope of this paper. In this section we wish to show representative effects of anisotropy and long range forces at triple lines using approximations and simplifications that render the equations tractable and provide insights on how nematic triple lines may differ from isotropic lines. More rigorous treatments will have to be performed in the future. Previous work in the area is found in [12]. In this section we present an application of the formalism to a large nematic lens (phase 1) bounded by two isotropic phases (phase 2 and phase 3). The triple line is a flat large circle. We assume that the lower phase 3 is very dense so that the nematic–phase 3 interface is flat. We assume constant and isotropic line energies. For a sufficiently large lens we can neglect line curvature. The nematic phase is uniaxial, and the scalar order parameter is unchanged and equal to its equilibrium value:

$$\mathbf{Q}=s_1^{\mathrm{eq}}(\mathbf{nn}-\mathbf{I}/3) \tag{73}$$

where s_1^{eq} minimizes f_{bh}. Thus only orientation contributions are taken into account. In addition we further simplify the energies by considering only first order anchoring effects and use the one-constant approximation in the bulk. The surface energies are $f_{sg}^{(1,2)}=f_{sg}^{(3,1)}=0, f_{sh}^{(2,3)}=f_{s\ \mathrm{iso}}^{(2,3)}$ and

$$f_{sh}^{(1,2)}=f_{s\ \mathrm{iso}}^{(1,2)}+f_{s\ \mathrm{an}}^{(1,2)},\quad f_{s\ \mathrm{an}}^{(1,2)}=\tilde{z}_{11}^{(1,2)}(\mathbf{n}\cdot\boldsymbol{\xi}^{(1,2)})^2, \tag{74a}$$

$$f_{sh}^{(3,1)}=f_{s\ \mathrm{iso}}^{(3,1)}+f_{s\ \mathrm{an}}^{(3,1)},\quad f_{s\ \mathrm{an}}^{(3,1)}=\tilde{z}_{11}^{(3,1)}(\mathbf{n}\cdot\boldsymbol{\xi}^{(3,1)})^2, \tag{74b}$$

where all scalar order parameter contributions have been absorbed into the remaining coefficients. When $\tilde{z}_{11}^{(i,j)}>0$ the surface energy favors tangential director orientation at the (ij) interface and when $\tilde{z}_{11}^{(i,j)}<0$ it favors orthogonal (homeotropic) orientation at the interface. The favored orientations that minimize surface energy are known as the easy axes. Under strong anchoring conditions bulk elastic energy is less costly and the director orients along the surface easy axis. Under weak anchoring conditions surface energy is less costly and bulk distortions are avoided. For systems bounded by different surfaces, hybrid conditions are possible. The bulk gradient energy in the one-constant approximation ($L_2=0$) used here is

$$f_{bg}=\frac{K}{2}(\nabla\mathbf{n}):(\nabla\mathbf{n})^T, \tag{75}$$

where $K=2L_1S^2$ is the Frank constant of elasticity. The principal geometric frame is $(\mathbf{t},\mathbf{p},\mathbf{b})=(\mathbf{t},\boldsymbol{\nu}^{(1,3)},\boldsymbol{\xi}^{(2,3)})$. The previously defined tangent and normal vectors to the interfaces at the triple line are $\boldsymbol{\nu}^{(2,3)}=-\boldsymbol{\nu}^{(3,1)}$, $\boldsymbol{\xi}^{(2,3)}=-\boldsymbol{\xi}^{(3,1)}$. The contact angle between the two nematic interfaces at the triple line is defined by $\cos\varsigma=\boldsymbol{\nu}^{(1,2)}\cdot\boldsymbol{\nu}^{(3,1)}=-\boldsymbol{\nu}^{(1,2)}\cdot\boldsymbol{\nu}^{(2,3)}$, and $\sin\varsigma=\boldsymbol{\xi}^{(1,2)}\cdot\boldsymbol{\nu}^{(2,3)}$. For simplicity we assume that $\tilde{z}_{11}^{(1,2)}=\tilde{z}_{11}^{(3,1)}>0$, and the easy axis at both surfaces is tangential. The two representative cases are (a) weak anchoring and (b) strong anchoring. Under weak anchoring conditions the role of interfacial anisotropy on nematic triple lines will be characterized. Under strong anchoring conditions the role of bulk long range elasticity on nematic triple lines will be characterized.

(a) Weak anchoring. The geometry and director field under weak anchoring are shown in Fig. 3. Under weak anchoring conditions, the characteristic thickness of the nematic region becomes smaller than the extrapolation length $K/\tilde{z}_{11}^{(i,j)}$ and bulk gradients vanish. Thus at finite distances $\ell<\ell_c=K/(\tilde{z}_{11}^{(1,2)}\tan\varsigma)$ the director field $\mathbf{n}$ is constant and given by $\mathbf{n}\cdot\boldsymbol{\nu}^{(1,2)}=\mathbf{n}\cdot\boldsymbol{\nu}^{(3,1)}=\cos(\varsigma/2)$. Since the director field is constant the bulk equations are satisfied. Since we assume that surface anchoring is negligible when compared to bulk elasticity, the interfacial equations are satisfied. Thus at the triple line the junction sum of stresses must vanish. In contrast to isotropic triple lines, the forces that act arise from normal and bending stresses. The anchoring energy contributes to both normal and bending stresses. The stress sum junction is therefore

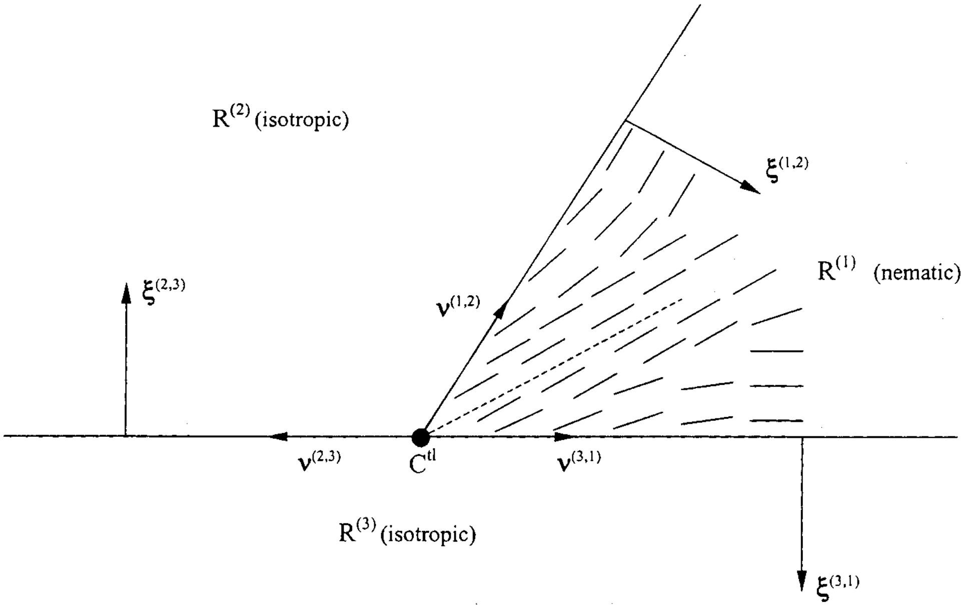

FIG. 3. Schematic of geometry and director field in the vicinity of a nematic triple line under weak anchoring conditions. The support bulk phase $R^{(3)}$ is assume to be very dense such that the bottom of the nematic lens is flat. It is assumed that the director field becomes homogeneous as the triple line is approached. Deviation from parallel surface orientation in the nematic phase ($R^{(1)}$) increases the anchoring energy and introduces bending stresses. Bending stress forces are normal to the interface and provide a mechanism to balance forces in all directions.

$$\sum_{\mathrm{jun}} \boldsymbol{\nu}\cdot\mathbf{T}_s = \underbrace{\boldsymbol{\nu}^{(1,2)} f_{s\ \mathrm{iso}}^{(1,2)} + \boldsymbol{\nu}^{(3,1)} f_{s\ \mathrm{iso}}^{(3,1)} + \boldsymbol{\nu}^{(2,3)} f_{s\ \mathrm{iso}}^{(2,3)}}_{\text{normal stress}} + \underbrace{\boldsymbol{\nu}^{(1,2)} f_{s\ \mathrm{an}}^{(1,2)} + \boldsymbol{\nu}^{(3,1)} f_{s\ \mathrm{an}}^{(3,1)}}_{\text{normal stress}} - \underbrace{\left\{ \boldsymbol{\nu}^{(1,2)} \frac{\partial f_{s\ \mathrm{an}}^{(1,2)}}{\partial \boldsymbol{\xi}^{(1,2)}} \boldsymbol{\xi}^{(1,2)} + \boldsymbol{\nu}^{(3,1)} \frac{\partial f_{s\ \mathrm{an}}^{(3,1)}}{\partial \boldsymbol{\xi}^{(3,1)}} \boldsymbol{\xi}^{(3,1)} \right\}}_{\text{bending stress}}, \tag{76}$$

showing that both tangential and normal forces arise through anchoring energy effects.

The **p** component of the triple line force balance equation gives the following generalized Neumann equation:

$$f_s^{(2,3)} = f_s^{(3,1)} + f_{s\ \mathrm{iso}}^{(1,2)} \cos\varsigma + \tilde{z}_{11}\left\{\left[\sin\left(\frac{\varsigma}{2}\right)\right]^2 (\cos\varsigma - 1) - \sin\varsigma^2\right\}, \tag{77}$$

showing that the effect of anchoring energy on the contact angle is due to bending and normal stresses. Using the **b** component of the force balance equation gives $f_{s\ \mathrm{iso}}^{(1,2)} = \tilde{z}_{11}[1 - \cos\varsigma - \sin(\varsigma/2)^2]$ and shows that the upper-directed force due to $f_{s\ \mathrm{iso}}^{(1,2)}$ is balanced by the downward anchoring force $\tilde{z}_{11}[1 - \cos\varsigma - \sin(\varsigma/2)^2]$. Combining the horizontal and vertical balances yields $f_{s\ \mathrm{iso}}^{(2,3)} = f_{s\ \mathrm{iso}}^{(3,1)} + \tilde{z}_{11}(6\cos\varsigma - 5 - \cos\varsigma^2)/4$, showing that in this case anchoring increases the contact angle. Partial wetting occurs whenever

$$0 < f_{s\ \mathrm{iso}}^{(3,1)} - f_{s\ \mathrm{iso}}^{(2,3)} < 3\tilde{z}_{11}, \tag{78}$$

showing that the upper threshold is a function of anchoring strength. Finally, the triple line torque balance equation is satisfied by the assumed constant director field.

(b) Strong anchoring. The geometry and director field under strong anchoring are shown in Fig. 4. Here we are concerned with a nematic wedge with a pure splay distortion in the proximity of the triple line, and wish to establish the range of long range bulk elasticity on the contact angle. Since the triple line coincides with a topological defect of strength $s = +1$, the long range effect is contained in the Peach-Koehler force $\mathbf{f}^{\mathrm{PK}}$ acting on the triple line:

$$\mathbf{F}^{\mathrm{PK}} = \oint_{\mathrm{jun}} (\mathbf{k}\cdot\mathbf{T}_b)\, d\ell. \tag{79}$$

Since we are using a director model in which a topological defect is singular we introduce a cutoff radius r_c of the size of the defect core and define the force by

$$\mathbf{F}^{\mathrm{PK}} = \lim_{\delta\to r_c} \int_{D_\delta^{(1)}} (\mathbf{k}\cdot\mathbf{T}_b^{(1)})\, d\ell. \tag{80}$$

Likewise, the junction couple integral at the triple line becomes

$$\oint_{\mathrm{jun}} (\mathbf{k}\cdot\mathbf{C}_b)\, d\ell = \lim_{\delta\to r_c} \int_{D_\delta^{(1)}} (\mathbf{k}\cdot\mathbf{C}_b^{(1)})\, d\ell. \tag{81}$$

Using the **Q** tensor model there is no need to introduce a cutoff since the topological defect becomes nonsingular. Also noncircular cores may introduce second order effects neglected here.

We use a cylindrical coordinate system (r,φ,z) attached to the triple line, with unit vectors $(\boldsymbol{\delta}_r, \boldsymbol{\delta}_\vartheta, \boldsymbol{\delta}_z)$ where φ is measured from $\nu^{(3,1)}$. The unit vector along the triple line is

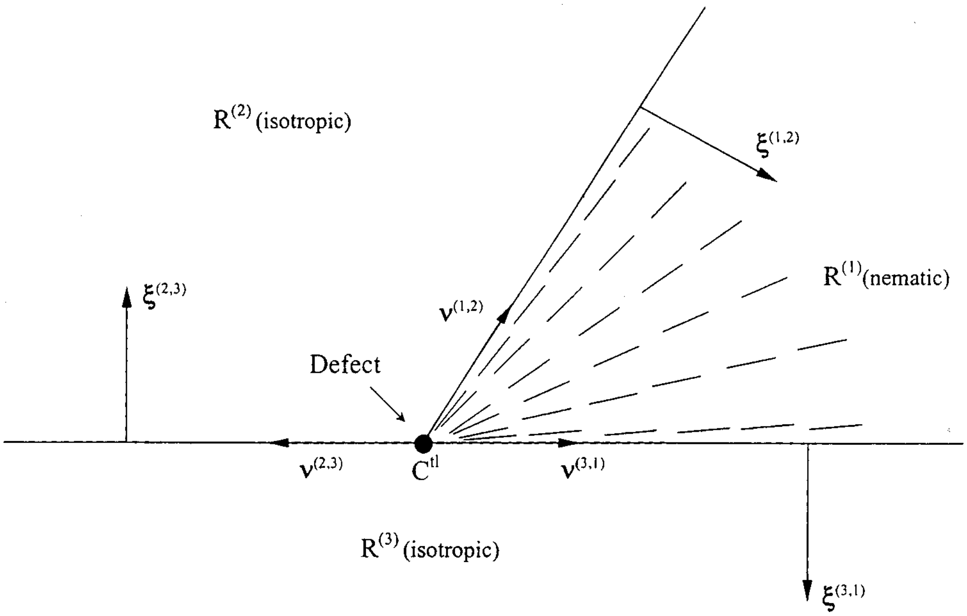

FIG. 4. Schematic of geometry and director field in the vicinity of a nematic triple line under strong anchoring conditions. The support bulk phase $R^{(3)}$ is assumed to be very dense such that the bottom of the nomadic lens is flat. It is assumed that the director field has a pure splay as the triple line is approached. The pure splay increases the bulk long range energy and produces a Peach-Koehler force that acts along the bisector and is directed away from the nematic phase.

$\mathbf{t}=-\delta_z$, and $\mathbf{k}=\delta_r$. In the cylindrical coordinate system the director field is planar: $\mathbf{n}=(\cos\theta,\sin\theta,0)$. In the bulk the director angle satisfies $\boldsymbol{\nabla}^2\theta=0$. A radially independent solution is $\theta=\vartheta$ and the corresponding bulk free energy density is $f_g=K/2r^2$. The corresponding stress vector $\mathbf{k}\cdot\mathbf{T}_b$ computed using Eq. (75) is purely radial, $\mathbf{k}\cdot\mathbf{T}_b=K/(2r^2)\delta_r$ and the corresponding stress couple vector $\mathbf{k}\cdot\mathbf{C}_b$ computed using Eq. (75) is equal to zero. The junction integrals therefore are

$$\mathbf{F}^{(\mathrm{PK})}=\int_{\varsigma}^{0}(\mathbf{k}\cdot\mathbf{T}_b)|_{r_c}r_c\,d\vartheta$$

$$=\frac{K}{2r_c}[-\sin\varsigma\,\boldsymbol{\nu}^{(3,1)}+(\cos\varsigma-1)\boldsymbol{\xi}^{(2,3)}],\qquad(82\mathrm{a})$$

$$\oint_{\mathrm{jun}}(\mathbf{k}\cdot\mathbf{C}_b)\,d\ell=0,\qquad(82\mathrm{b})$$

indicating the presence of horizontal and vertical forces and absence of torques. The force $\mathbf{F}^{\mathrm{PK}}$ acts along the bisector and away from the nematic phase:

$$\mathbf{F}^{\mathrm{PK}}=\frac{K}{2r_c}[-\sin\varsigma\;\boldsymbol{\nu}^{(3,1)}+(\cos\varsigma-1)\boldsymbol{\xi}^{(2,3)}]$$

$$=-\frac{K}{r_c}\sin\left(\frac{\varsigma}{2}\right)\left[\cos\left(\frac{\varsigma}{2}\right)\boldsymbol{\nu}^{(3,1)}+\sin\left(\frac{\varsigma}{2}\right)\boldsymbol{\xi}^{(2,3)}\right]\qquad(83)$$

The presence of a downward vertical force eliminates the inconsistency that arises when using the Young-Neumann contact angle equation and the supporting material is considered rigid and inelastic [9]. In that case the vertical forces are unbalanced. In the present model long range elasticity provides a balancing force to capillary forces. The components of the force balance equations at the triple line then become

$$\mathbf{t}\cdot\left(\oint_{\mathrm{jun}}(\mathbf{k}\cdot\mathbf{T}_b)\,d\ell\right)=0,\qquad(84\mathrm{a})$$

$$\mathbf{p}\cdot\left(\boldsymbol{\nu}^{(1,2)}f_{s\ \mathrm{iso}}^{(1,2)}+\boldsymbol{\nu}^{(3,1)}f_{s\ \mathrm{iso}}^{(3,1)}+\boldsymbol{\nu}^{(2,3)}f_{s\ \mathrm{iso}}^{(2,3)}\right.$$
$$\left.-\frac{K}{2r_c}[\sin\varsigma\;\boldsymbol{\nu}^{(3,1)}+(1-\cos\varsigma)\boldsymbol{\xi}^{(2,3)}]\right)=0,\qquad(84\mathrm{b})$$

$$\mathbf{b}\cdot\left(\boldsymbol{\nu}^{(1,2)}\mathbf{f}_{s\ \mathrm{iso}}^{(1,2)}+\boldsymbol{\nu}^{(3,1)}\mathbf{f}_{s\ \mathrm{iso}}^{(3,1)}+\boldsymbol{\nu}^{(2,3)}\mathbf{f}_{s\ \mathrm{iso}}^{(2,3)}\right.$$
$$\left.-\frac{K}{2r_c}[\sin\varsigma\;\boldsymbol{\nu}^{(3,1)}+(1-\cos\varsigma)\boldsymbol{\xi}^{(2,3)}]\right)=0.\qquad(84\mathrm{c})$$

The horizontal projection leads to

$$f_{s\ \mathrm{iso}}^{(1,2)}\cos\varsigma+f_{s\ \mathrm{iso}}^{(3,1)}-f_{s\ \mathrm{iso}}^{(2,3)}-\frac{K}{2r_c}\sin\varsigma=0\qquad(85)$$

and shows that the long range force increases with contact angle and is directed away from the nematic phase. The vertical projection leads to

$$f_{s\ \mathrm{iso}}^{(1,2)}\sin\varsigma-\frac{K}{2r_c}(1-\cos\varsigma)=0\qquad(86)$$

and shows that the long range force increases with contact angle, and how the surface tension force is balanced by the long range Peach-Koehler force [28]. Combination of both force balances leads to

$$f_{s\ \mathrm{iso}}^{(1,2)}+(f_{s\ \mathrm{iso}}^{(3,1)}-f_{s\ \mathrm{iso}}^{(2,3)})\cos\varsigma-\frac{K}{2r_c}\sin\varsigma=0.\qquad(87)$$

The partial wetting limits are thus independent of long range effects:

$$-1<\frac{f_{s\ \mathrm{iso}}^{(1,2)}}{(f_{s\ \mathrm{iso}}^{(3,2)}-f_{s\ \mathrm{iso}}^{(3,1)})}<1, \tag{88}$$

and the contact angle for partial wetting is

$$\tan\frac{\varsigma}{2}-\frac{K/2r_c+\sqrt{(K/2r_c)^2-[(f_{s\ \mathrm{iso}}^{(1,2)})^2-(f_{s\ \mathrm{iso}}^{(2,3)}-f_{s\ \mathrm{iso}}^{(3,1)})^2]}}{(f_{s\ \mathrm{iso}}^{(1,2)})-(f_{s\ \mathrm{iso}}^{(2,3)}-f_{s\ \mathrm{iso}}^{(3,1)})}. \tag{89}$$

If $(f_{s\ \mathrm{iso}}^{(3,1)}-f_{s\ \mathrm{iso}}^{(2,3)})=0$ there is partial wetting driven by long range elasticity if

$$-1<\frac{2\,f_{s\ \mathrm{iso}}^{(1,2)}r_c}{K}<1 \tag{90}$$

and the contact angle is

$$\sin\varsigma=\frac{2\,f_{s\ \mathrm{iso}}^{(1,2)}r_c}{K}. \tag{91}$$

The one-constant approximation in the bulk gradient energy eliminates a number of effects that may be present when the anchoring conditions are of the hybrid type, involving splay and bend. In addition, cases with escaped cores or noncircular cores may reduce or change the nature of the long range forces.

V. CONCLUSIONS

The Landau–de Gennes model for nematic liquid crystal bulk and interfaces has been extended to nematic triple lines, involving the intersection of two isotropic and one nematic phase. A complete set of bulk, interface, and triple line force and torque balance equations has been formulated using a systematic approach that takes into account homogeneous and long range bulk, surface, and line energies. Force and torque balances at the triple line contain lineal, interfacial, and bulk contributions. The interfacial contributions at the triple line appear as junction sums, while the bulk contributions appear as junction integrals. It is shown that the junction sums of interfacial stresses and torques and junction integrals of bulk stresses and torques are the lineal analogs of the well-known interface jumps of bulk stresses and torques. In the absence of gradient energies the equations are shown to reduce to the classical Neumann force balance at a fluid triple line. The structure of the force balance equations in terms of bulk, surface, and line stresses and torques is shown to follow from their dimensionality. A Landau–de Gennes free energy density for nematic lines is derived and used to formulate line stress and line torque equations. The nature of line stresses and line torque equations is revealed by identifying normal, distortion, and bending components. Normal line stresses are 1D analogs of pressure in 3D and surface tension in 2D, line distortion stresses are 1D analogs of the Ericksen stresses in 2D and 3D, and line bending stresses are 1D analogs of surface bending stresses in 2D. Similarly, the correspondence between lineal, areal, and bulk torques is established.

Projection of the balance equations along the Frenet-Serret triple line frame shows which of the stress and torque components balance in the principal frame. Applications of the model to the contact angle of a nematic lense between two fluids show that interfacial anchoring and bulk gradient energy modify the classical results. Under weak anchoring the main effect on the triple line is due to interfacial anchoring (anisotropy) effects, while under strong anchoring the main effects on the triple line are due to bulk long range contributions. Lack of force balance at a triple line due to lack of long range forces and anisotropic effects is removed and a consistent formulation is shown to emerge. More rigorous applications of the balance equations as well as other line free energies of nematic contact lines will predict a range of other phenomena not discussed here.

ACKNOWLEDGMENTS

This work was supported by a grant from the Donors of The Petroleum Research Fund (PRF) administered by the American Chemical Society. This research was supported in part by the National Science Foundation under Grant No. PHY99-07949.

[1] A. A. Sonin, *The Surface Physics of Liquid Crystals* (Gordon and Breach, Amsterdam, 1995).
[2] B. Jerome, in *Handbook of Liquid Crystals*, edited by D. Demus, J. Goodby, G. W. Gray, H.-W. Spiess, and V. Vill (Wiley-VCH, Weinheim, 1998), Vol. 1.
[3] H. Yokoyama, in *Handbook of Liquid Crystal Research*, edited by P. J. Collins and J. S. Patel (Oxford University Press, New York, 1997), Chap. 6, p. 179.
[4] T. J. Sluckin and A. Poniewierski, in *Fluid Interfacial Phenomena*, edited by C. A. Croxton (Wiley, Chichester, 1986), Chap. 5.
[5] M. A. Osipov and S. Hess, J. Chem. Phys. **99**, 4181 (1993).
[6] E. G. Virga, *Variational Theories for Liquid Crystals* (Chapman and Hall, London, 1994).
[7] G. Barbero and G. Durand, in *Liquid Crystals in Complex Geometries*, edited by G. P. Crawford and S. Zumer (Taylor and Francis, London, 1996), p. 21.
[8] D. A. Edwards, H. Brenner, and D. T. Wasan, *Interfacial Transport Processes and Rheology* (Butterworth, Boston, MA, 1991).
[9] J. C. Slattery, *Interfacial Transport Phenomena* (Springer-Verlag, New York, 1990).
[10] A. Poniewierski, Liq. Cryst. **27**, 1369 (2000).
[11] A. D. Rey, Phys. Rev. E **61**, 1540 (2000).
[12] A. D. Rey, J. Chem. Phys. **110**, 9769 (1999).
[13] A. D. Rey, Liq. Cryst. **28**, 549 (2001).
[14] P. G. de Gennes and J. Prost, *The Physics of Liquid Crystals*, 2nd ed. (Oxford University Press, London, 1993).
[15] D. W. Hoffman and J. W. Cahn, Surf. Sci. **31**, 368 (1972).
[16] J. W. Cahn and D. W. Hoffman, Acta Metall. **22**, 1205 (1974).

[17] D. J. Steigmann, Arch. Ration. Mech. Anal. **150**, 127 (1999).
[18] H. Garcke, B. Nestler, and B. Stoth, Physica D **115**, 87 (1997).
[19] C. Papenfuss and W. Muschik, Mol. Mater. **2**, 1 (1992); Mol. Cryst. Liq. Cryst. Sci. Technol., Sect. A **262**, 473 (1995); Phys. Rev. E **56**, 4275 (1997).
[20] J. T. Jenkins and P. J. Barrat, Q. J. Mech. Appl. Math. **27**, 111 (1974).
[21] A. K. Sen and D. E. Sullivan, Phys. Rev. A **35**, 1391 (1987).
[22] J. O. Indekeu, Int. J. Mod. Phys. B **8**, 309 (1994).
[23] H. Dobbs, Physica A **271**, 36 (1999).
[24] S. Faetti, in *Physics of Liquid Crystalline Materials*, edited by I.-C. Khoo and F. Simoni (Gordon and Breach, Philadelphia, 1991), Chap. 12, p. 301.
[25] M. Vignes-Adler and H. Brenner, J. Colloid Interface Sci. **103**, 11 (1985).
[26] E. F. Gramsbergen, L. Longa, and W. H. de Jeu, Phys. Rep. **135**, 195 (1986).
[27] N. K. Simha and K. Bhattacharya, J. Mech. Phys. Solids **46**, 2323 (1998).
[28] F. R. N. Nabarro, *Theory of Crystal Dislocations* (Dover, New York, 1987).